J. metamorphic Geol., 1998, **16,** 149–167

SHRIMP monazite and zircon geochronology of high-grade metamorphism in New Zealand

T. R. IRELAND[1] AND G. M. GIBSON[2]*
[1]*Research School of Earth Sciences, Australian National University, Canberra ACT 0200, Australia (email: trevor.ireland@anu.edu.au)*
[2]*Department of Applied Sciences, University of Southern Queensland, Toowoomba, QLD 4350 Australia*

ABSTRACT Ion microprobe dating of zircon and monazite from high-grade gneisses has been used to (1) determine the timing of metamorphism in the Western Province of New Zealand, and (2) constrain the age of the protoliths from which the metamorphic rocks were derived. The Western Province comprises Westland, where mainly upper crustal rocks are exposed, and Fiordland, where middle to lower crustal levels crop out. In Westland, the oldest recognisable metamorphic event occurred at 360–370 Ma, penecontemporaneously with intrusion of the mid-Palaeozoic Karamea Batholith (*c.* 375 Ma). Metamorphism took place under low-pressure/high-temperature conditions, resulting in upper-amphibolite sillimanite-grade metamorphism of Lower Palaeozoic pelites (Greenland Group). Orthogneisses of younger (Cretaceous) age formed during emplacement of the Rahu Suite granite intrusives (*c.* 110 Ma) and were derived from protoliths including Cretaceous Separation Point suite and Devonian Karamea suite granites. In Fiordland, high-grade paragneisses with Greenland Group zircon age patterns were metamorphosed (M1) to sillimanite grade at 360 Ma. Concomitant with crustal thickening and further granite emplacement, M1 mineral assemblages were overprinted by higher-pressure kyanite-grade metamorphism (M2) at 330 Ma. It remains unclear whether the M2 event in Fiordland was primarily due to tectonic burial, as suggested by regional recumbent isoclinal folding, or whether it was due to magmatic loading, in keeping with the significant volumes of granite magma intruded at higher structural levels in the formerly contiguous Westland region. Metamorphism in Fiordland accompanied and outlasted emplacement of the Western Fiordland Orthogneiss (WFO) at 110–125 Ma. The WFO equilibrated under granulite facies conditions, whereas cover rocks underwent more limited recrystallization except for high-strain shear zones where conditions of lower to middle amphibolite facies were met. The juxtaposition of Palaeozoic kyanite-grade rocks against Cretaceous WFO granulites resulted from late Mesozoic extensional deformation and development of metamorphic core complexes in the Western Province.

Key words: Fiordland; monazite; New Zealand; U–Th–Pb geochronology; zircon.

INTRODUCTION

Deciphering the geochronology of complex metamorphic terranes remains a di cult task, despite the advances in geochronological techniques. In part this is due to the overprinting of pre-existing assemblages by successive metamorphic event(s) and the partial or complete resetting of geochronometers, such as K–Ar, Ar–Ar and Rb–Sr, in high-grade events. Ion microprobe dating of zircon has been important in this respect, because zircon is very resilient to resetting, and sequential overgrowths can record a history of events provided temperatures are high enough to precipitate new zircon overgrowths. Although intermediate-high pressure, low-medium temperature metamorphism (Barrovian) does not always result in new zircon growth, monazite is a common accessory mineral forming from prograde metamorphism of pelitic compositions (Parrish, 1990; Smith & Barreiro, 1990; Kingsbury *et al*., 1993). Thus, having both zircon and monazite geochronology available with the ion microprobe presents new possibilities in the dating and characterization of high-grade metamorphic terranes.

The subject of this study is metamorphism in the Western Province of New Zealand (Fig. 1). The high-grade metamorphic rocks of this region, first documented by Turner (1937a,b, 1938) and used as case studies in his classic texts on metamorphic petrology (Williams *et al*., 1954; Turner, 1968), have been the source of much study and discussion. The nature of Fiordland metamorphic rocks has been examined in several Otago University PhD theses and these have been elegantly summarized by Brown (1996). Notwithstanding the volume of detailed petrological work carried out on Western Province gneisses and the tectonic implications ascribed to them, very little

**Present address*: Australian Geological Survey Organisation, Canberra ACT 2601, Australia.

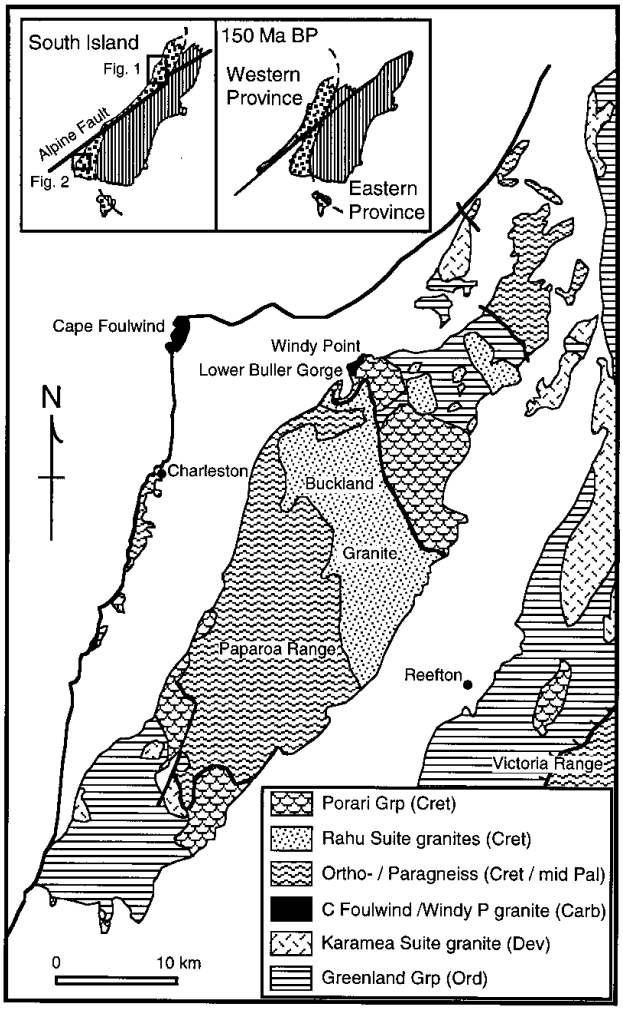

Fig. 1. Geology of Westland region where ortho- and paragneisses are exposed. The inset illustrates the contiguity of Westland and Fiordland prior to displacement along the Alpine Fault. Areas delineated for Figs 1 & 2 are also shown in inset. Adapted from Tulloch & Palmer (1990).

geochronology has been carried out to support the various tectonic models proposed for the region.

Discussion on the age and tectonic setting of metamorphism in the metasedimentary rocks (Tuhua sequence), comprising much of central and western Fiordland, has been based primarily on limited K–Ar ages, despite the susceptibility of this system to resetting (e.g. Aronson, 1968). Landis & Coombs (1967) and Bradshaw (1989) favoured a late Mesozoic age for metamorphism of the metasediments, whereas others (e.g. Oliver, 1980; Gibson *et al.*, 1988; 1989) considered metamorphism to be mid-Palaeozoic. Based on Palaeozoic K–Ar ages, Gibson *et al.* (1988) interpreted Fiordland as an analogue of a metamorphic core complex with an upper plate composed mainly of metasediments metamorphosed during the mid-Palaeozoic Tuhua orogeny and a lower plate represented by the Western Fiordland Orthogneiss (WFO), consisting mainly of Early Cretaceous granulites (Mattinson *et al.*, 1986; Gibson *et al.*, 1988; Gibson & Ireland, 1995). In the view of Gibson and co-workers, metamorphism and deformation in the upper and lower plates occurred at di erent times. On the other hand, Bradshaw (1989) argued that metamorphism of the metasediments and granulites occurred contemporaneously. A similar interpretation has been pro ered by Brown (1996), who attributed high-pressure metamorphism in the country rock to magmatic loading associated with emplacement of the WFO.

Orthogneisses and paragneisses also occur on the opposite side of the Alpine Fault in Westland. Orthogneiss from Constant Bay near Charleston was once regarded as Precambrian and thus the oldest rock unit in New Zealand (Adams, 1975), but U–Pb zircon dating (Kimbrough & Tulloch, 1989) has revealed a Cretaceous metamorphism responsible for orthogneiss formation. However, there is still considerable controversy about the nature of the protolith for the paragneisses and whether this has a Precambrian origin (Tulloch & Kimbrough, 1989; White, 1994).

In this paper we report ion microprobe (SHRIMP) data from zircon and monazite separated from Western Province gneisses from Westland and Fiordland. These data are used to determine the chronology of metamorphism in the Western Province and constrain the age(s) of the protoliths of the metamorphic rocks. Determination of a chronology for metamorphism has implications not only for crustal evolution in New Zealand, but for the Pacific margin of Gondwana as a whole. Indeed, New Zealand is one of the few locations along this former plate margin where a near complete section through the continental crust is exposed.

REGIONAL GEOLOGY AND GEOCHRONOLOGY

The Western Province of New Zealand comprises Westland/Nelson and the formerly contiguous region of Fiordland, which is now o set from the Westland/Nelson area by 500 km of movement along the late Tertiary Alpine Fault (Fig. 1).

Nelson–Westland

The main units in Nelson and Westland are weakly metamorphosed lower-Palaeozoic sedimentary rocks and volcanic sequences of the Buller and Takaka terranes intruded by mid-Palaeozoic granites and minor gabbro (Cooper, 1989; Fig. 1). High-grade gneisses are exposed at Charleston, in the Paparoa Range, and in the Victoria Range, where low-angle detachment faults bring the gneisses into contact with low-grade sediments and intrusive rocks. These features have been interpreted as those of a metamorphic core complex formed during extension associated with the

initiation of the Cretaceous break-up at the Gondwana margin (Tulloch & Kimbrough, 1989).

The main sedimentary unit in the basement of Westland is the Ordovician Greenland Group, which consists predominantly of flysch metamorphosed to greenschist facies. The Greenland Group is intruded by Palaeozoic and Mesozoic granites. The Karamea Batholith constitutes the largest intrusive suite in the region, and recent ion probe dating has firmly established a relatively short-lived intrusive period of around 370–380 Ma (zircon U–Pb ion probe, Muir *et al*., 1994; 1996a). Individual plutons from the Karamea Batholith vary substantially in their chemistry which is primarily a result of mixing of the primary magmas with varying amounts of Greenland Group sediment (Muir *et al*., 1996b). Two plutons at Cape Foulwind and Windy Point (Fig. 1) have Carboniferous ages (*c*. 330 Ma, zircon U–Pb ion probe, Muir *et al*., 1994) and are highly chemically fractionated compared to the Karamea intrusives.

Two temporally overlapping episodes of Cretaceous granite magmatism are present in western New Zealand. The Separation Point Batholith (SPB) has the chemistry of convergent plate magmatism (Muir *et al*., 1995), and stitches the Eastern and Western Provinces of New Zealand together (Kimbrough *et al*., 1993). Isolated plutons of SPB are also present throughout the Western Province (Muir *et al*., 1994; 1997). Separation Point Batholith plutons have a restricted age range of 111–118 Ma (K–Ar, Harrison & McDougall, 1980; zircon U–Pb TIMS, Kimbrough *et al*., 1993, 1994, zircon U–Pb ion probe, Muir *et al*., 1994). Granitic rocks of the Rahu Suite (Tulloch, 1983) occur as plutons scattered down the West Coast. These granites contain a large fraction of inherited zircon (predominantly Greenland Group detrital zircon) and also have a restricted age range of 110–115 Ma (zircon U–Pb ion probe, Waight *et al*., 1997). The largest of the Rahu Suite plutons, the Buckland Granite has an age of 109.6 ± 1.7 Ma (zircon U–Pb ion probe, Muir *et al*., 1994). The youngest Cretaceous granite is the French Creek granite dated at *c*. 83 Ma (zircon U–Pb TIMS, Tulloch *et al*., 1994; zircon U–Pb ion probe, Waight *et al*., 1997).

The metamorphic core complexes represent a tectonic window to mid crustal levels on the West Coast. The Charleston gneisses have alternatively been viewed as Precambrian basement to the Greenland Group sediments (e.g. Nathan, 1976), or as having formed from metamorphism of Greenland Group (Laird, 1967). The former interpretation was supported by a Rb–Sr isochron yielding an age of 680 ± 21 Ma, with a satisfactory MSWD of 2.1 (Adams, 1975), which precludes the Ordovician Greenland Group as a protolith for the gneisses. However, Kimbrough & Tulloch (1989) subsequently analysed zircon splits from four Charleston orthogneisses, as well as one paragneiss (in order to constrain the extent to which the orthogneisses were contaminated with possible metasedimentary material). Their data are dispersed along a mixing line, with the orthogneisses close to the lower intercept at 114 ± 18 Ma. However, the line-fit has a large MSWD of 1380, indicating that the data cannot be represented by simple mixing of the Cretaceous orthogneisses with a component at the upper intercept age of 1097 ± 200 Ma. The clustering of the orthogneisses close to the lower intercept establishes a Cretaceous origin for the orthogneisses, but resolution of the components responsible for the high degree of scatter is important in terms of constraining the protoliths of the gneisses. Furthermore, the age of metamorphism of the paragneisses has not been addressed.

Fiordland

Fiordland has been divided into western, central and eastern belts and a southwest-Fiordland block (Oliver & Coggon, 1979). Like Westland, the eastern belt and southwest block encompass weakly metamorphosed sedimentary rocks intruded by Palaeozoic and Mesozoic granites. In contrast, central and western Fiordland are composed of rocks metamorphosed at amphibolite and granulite facies (Fig. 2). Granulite facies rocks are represented by the Cretaceous Western Fiordland Orthogneiss (WFO; Bradshaw, 1989, 1990) and include both two-pyroxene and higher pressure garnet varieties (Oliver & Coggon, 1979; Bradshaw, 1989; Gibson & Ireland, 1995). These rocks were derived from Early Cretaceous plutonic protoliths with

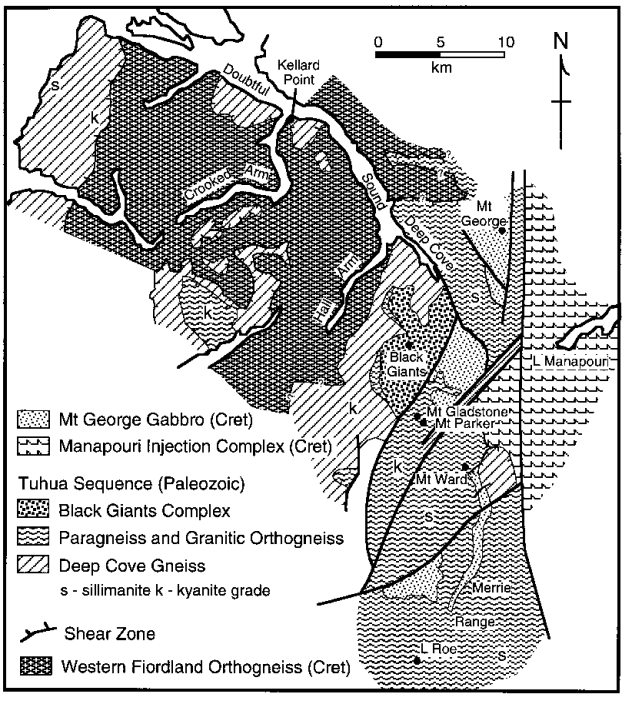

Fig. 2. Geology of Fiordland region between the southwest arm of Lake Manapouri and Doubtful Sound. Adapted from Gibson (1990).

U–Pb zircon ages in a restricted range from around 116–125 Ma (Mattinson *et al*., 1986; Gibson *et al*., 1988) with some granulite as young as 108 ± 3 Ma (zircon U–Pb ion probe, Gibson & Ireland, 1995). The chemistry of the WFO is distinctive and the same as that of the Separation Point Batholith and, together with the similarity in ages, suggests that the WFO is the metamorphosed root zone of the SPB (Muir *et al*., 1995).

The WFO is structurally overlain by a much older, multiply deformed (D1–D4) Cambro-Ordovician sequence (Tuhua sequence) metamorphosed to amphibolite facies. Mineral assemblages in the Tuhua sequence record evidence of two quite separate metamorphic events: the first (M1) of low-*P* to high-*T* producing widespread sillimanite-K-feldspar $\pm$ cordierite assemblages in rocks of appropriate composition, whereas the second (M2) produced Barrovian-style, medium pressure assemblages containing garnet, kyanite, rutile and occasionally K-feldspar as well as staurolite and/or muscovite. Low-*P* to high-*T* metamorphism outlasted the D1 deformational event and at the higher structural levels continued during D2. On the other hand, Barrovian metamorphism is syn- to post-D2 in age and is largely confined to the deeper levels of the Tuhua Sequence. Folds produced during D1 and D2 deformation are tight to isoclinal and generally recumbent with well-developed axial plane schistosities (Oliver, 1980; Gibson, 1982; 1992).

Following D2 deformation, rocks of the Tuhua sequence were subject to decompression and rapid uplift attendant on the D3 deformation. This event also a ected the WFO and is thought (Gibson *et al*., 1988) to have been induced by continental extension and the processes leading to the opening of the Tasman Sea. A second phase of granulite facies metamorphism related to this event has been dated at 108 ± 3 Ma (Gibson & Ireland, 1995). However, by late Mesozoic time cooling was well advanced, as evidenced by a 93 Ma hornblende age derived from a D3 mylonite (Gibson *et al*., 1988). Actual exhumation of the granulites and deeper structural levels of the Tuhua sequence did not occur until the onset of D4 deformation, when there was a marked change in motion along the late Tertiary Alpine Fault from dominantly strike-slip to dominantly reverse-slip. This change led to renewed uplift in Fiordland and produced the dome-like structure that characterises the region today.

The Tuhua sequence is in low-angle fault contact with the granulites (Oliver & Coggon, 1979; Gibson *et al*., 1988; Hill, 1995) and a core-complex model was proposed (coincidentally at the same time as the core complex model for Westland; Tulloch & Kimbrough, 1989) to account for the major structural features of Fiordland (Gibson *et al*., 1988) and the preservation of Palaeozoic K–Ar ages in the Tuhua sequence. However, in light of the Cretaceous age of granulite metamorphism of the WFO, Bradshaw (1990) proposed that the high-grade metamorphic assemblages in the Tuhua sequence were also produced in the Cretaceous. In his view, sillimanite-grade rocks were thermally metamorphosed by the Western Fiordland Orthogneiss and then both Tuhua sequence and WFO were taken to deeper crustal levels and higher pressures where kyanite stabilised in the Tuhua sequence. Bradshaw & Kimbrough (1989) discounted crustal extension in Fiordland, because the high-grade upper plate in the Fiordland metamorphic core complex is not identical to the low-grade metasedimentary rocks encountered in more typical core complexes, such as in the Basin and Range Province of western USA. Subsequently, Brown (1996) interpreted the kyanite-grade rocks adjacent to the Cretaceous WFO as a metamorphic aureole developed during emplacement of the granulite protolith.

In contrast, Gibson *et al*. (1989) and Gibson (1990) argued that juxtaposition is the result of deformation accompanying late-Mesozoic continental extension; the WFO and deeper structural levels of Tuhua sequence are exposed in a tectonic window in the upper plate. As with core complexes elsewhere, cover rocks in Fiordland are separated from lower plate rocks by a major low-angle detachment surface of extensional origin (Gibson *et al*., 1988; Hill, 1995). On approach to this detachment surface, sillimanite gives way to kyanite in metapelitic assemblages consistent with increased depths of burial in the Tuhua sequence (Gibson *et al*., 1988). Notwithstanding uncertainties in the timing of kyanite-grade metamorphism, Fiordland underwent major orogenesis in both mid-Palaeozoic and late Mesozoic times.

SAMPLES

The samples analysed are listed in Table 1. Samples were chosen to address the following issues: (1) nature and protolith of ortho- and paragneisses, and (2) their metamorphic ages.

Point 1 is addressed by the zircon age spectra. The age spectra of the metasediments have implications for the development of the Gondwana margin, but a complete discussion of these data is not within the scope of the present work. The age spectra are solely used for distinguishing potential protoliths.

Point 2 is addressed by dating monazites formed during prograde metamorphism of metapelites.

Field samples, typically weighing 0.5–1 kg, were reduced to clean chips, which were then washed and crushed. Mineral separation was carried out with standard heavy liquid and magnetic separation techniques. Zircons and monazites were mounted in epoxy resin and polished to expose their midsections. Because biasing can be induced by sample selection, hand-picking was limited to removal of extraneous material. For a zircon age spectrum, all zircons on a given photomicrograph were analysed, regardless of size or morphology, so that no operator selection was involved. In this way, we infer that the detrital zircons are largely unbiased representatives of the zircon population in the rock. For geochronology, a variety of clean grains was selected, but the fraction mounted also contains unbiased material, so that all morphologies are represented.

ANALYTICAL TECHNIQUES

Zircon and monazite were analysed with the SHRIMP I and II ion microprobes at ANU. The techniques used for zircon analysis are

Table 1. Sample localities and details.

Sample	No.	Map ref.	M	Z	Other information
Westland					
Buckland Granite	RNZ119	S37/196613	√	1	Lower Buller Gorge
Dunphy Granite	94-149	L29/286326	√	2	Bens Bridge, Upper Buller Gorge
Charleston Orthogneiss	P45042		×	√ 3	
Charleston Orthogneiss	90-428	S30/941544	√	√	Porphyritic, Constant Bay
Charleston Paragneiss	90-427	S30/950550	√	√	Nile River
Victoria Range Paragneiss	90-423	L30/222902	√	√ 4	Rough Stream
Greenland Group	90-444	S57/433320	×	√	Greywacke, Mt. Greenland, near Ross
Greenland Group	90-430	S38/352223	×	√	Greywacke, Globe Mine, south of Reefton
Fiordland					
Lake Roe Schist	91-586	S157/307835	√	√ 5	Sillimanite-bearing, L. Roe Merrie Range
Lake Roe Psammite	91-587	S157/310837	√	×	Sillimanite-bearing, L. Roe Merrie Range
Mt. Gladstone Schist	94-188	S148/238005	√	√	Kyanite-bearing, Mt Gladstone
Mt Parker Schist	91-585	S148/281990	√	×	Kyanite-bearing, Mt Parker
Deep Cove Gneiss	95-299	S139/178244	×	√	Kellard Point, Crooked Arm
Deep Cove Gneiss	91-589	S139/167236	×	5	Kellard Point, Crooked Arm
Orthogneiss	95-300	S148/223040	×	√	Discordant intrusive in kyanite schist
Orthogneiss	95-301	S148/224054	×	5	Intrusive in kyanite schist

M √ = monazite analysed, Z √ = zircon analysed in this work and/or by reference:.
[1] Muir *et al.* (1994); [2] Muir *et al.* (1996); [3] Kimbrough & Tulloch (1989); [4] Ireland (1992); [5] Gibson & Ireland (1996).

described in Muir *et al.* (1996a). Zircon analyses in this work are mainly used to obtain detrital zircon age spectra and for these we used $^{204}Pb/^{206}Pb$ to estimate the common Pb component. For the age determinations of zircon in the orthogneisses, common Pb was based on the $^{207}Pb/^{206}Pb$ ratio predicted for a concordant datum, with a common Pb isotopic composition given by the Cumming & Richards (1975) Pb growth model for the inferred age. U/Pb was normalized to 0.0928 for the 572 Ma SL13 standard using an empirical quadratic calibration of the form $Pb/U = a(UO/U)^2$). For the metasediments, ages are based on the weighted mean $^{206}Pb/^{238}U$ and $^{207}Pb/^{206}Pb$ ages for near concordant zircons. For discordant zircons, the $^{206}Pb/^{238}U$ age was used when it was less than 800 Ma, while the $^{207}Pb/^{206}Pb$ age was used for zircons with $^{206}Pb/^{238}U$ ages older than 800Ma. For the orthogneisses, weighted means of the $^{206}Pb/^{238}U$ ages were used, with rejection of outliers based on the MSWD for the appropriate number of degrees of freedom.

The techniques used for monazite dating are broadly similar to zircon and are described in detail in Appendix A. Briefly, U/Pb and Th/Pb ratios were normalized to 0.06749 and 0.02105, respectively, for the 421 Ma monazite from the Ma ra Adamellite with independent quadratic calibrations for Pb/U [vs. $(UO/U)^2$] and Pb/Th [vs. $(ThO/Th)^2$]. The estimated common Pb contribution was based on the $^{207}Pb/^{206}Pb$ ratio predicted for a concordant datum.

Because U/Pb and Th/Pb ages are determined relative to the mean of the standard zircon or monazite, the error in the weighted mean age of the standard is summed in quadrature with that for the unknown to obtain the final error in the age (of the unknown).

All age data are plotted on cumulative probability diagrams of U–Pb ages (and also Th–Pb ages for monazite). The cumulative probability data are calculated by taking the individual data points and assuming a Gaussian distribution of unit area with width proportional to the error, and summing these for all data in 1 Ma bins over the time interval of interest. The cumulative probability plots are essentially histograms for the data allowing for the errors of individual points.

The techniques for measuring U–Th–Pb ages from monazites were tested by analysing monazites from granites, the ages of which had been obtained through their magmatic zircon. Two granites were chosen from the Western Province, the Cretaceous Buckland Granite (109.6 ± 1.7 Ma; U–Pb zircon age, Muir *et al.*, 1994) and the Palaeozoic Dunphy Granite (375.4 ± 5.6 Ma; U–Pb zircon age, Muir *et al.*, 1996a). Both of these granites show marked zircon inheritance from the surrounding Greenland Group sediments (Muir *et al.*, 1994, 1996a) and contain abundant monazite. Data for these two samples are given in Table 2; data from the other samples are available from the authors on request.

A cumulative-probability diagram for Buckland monazite is shown in Fig. 3a. The 20 U–Pb analyses show excess scatter (MSWD = 2.0), but after rejecting one low point, a satisfactory MSWD of 1.62 and a weighted mean age of 110 ± 2 Ma ($2\sigma_m$) was obtained. The MSWD of the 20 Th–Pb analyses is only marginally high at 1.9, but one point lies nearly 4σ above the mean. Rejecting this point gives a MSWD of 1.08 and a final age of 111 ± 2 Ma ($2\sigma_m$). The U–Pb and Th–Pb ages agree within error and are also within error of the zircon U–Pb age (109.6 ± 1.7 Ma; Muir *et al.*, 1994). Th/U ratios range from 4 to 60, most grains having Th/U less than 20. The fraction of common ^{206}Pb (out of the total measured Pb; $f^{206}Pb$) varies inversely with the U concentration, but is still less than 2.5% in all cases.

Nineteen analyses were made of monazites from the Dunphy Granite, and the cumulative-probability diagram is shown in Fig. 3b. One marginally low U–Pb point has been rejected, and the MSWD of the U–Pb mean is then 0.75 and the weighted mean age is 370 ± 8 Ma ($2\sigma_m$). Two low-precision Th–Pb ages have been excluded, and the remaining 17 Th–Pb measurements give an MSWD of 0.67 and a weighted mean age of 377 ± 8 Ma ($2\sigma_m$). These ages are within error of each other and are also in good agreement with the zircon age of the Dunphy granite of 375.4 ± 5.6 Ma (Muir *et al.*, 1996a).

The monazite data for both Buckland and Dunphy granites are within error of their respective zircon ages which indicates internal consistency between $^{206}Pb/^{238}U$ zircon and $^{206}Pb/^{238}U$ and $^{208}Pb/^{232}Th$ monazite dating schemes for zircons and monazites ranging in age between 100–400 Ma.

GEOCHRONOLOGY

Sedimentary and metasedimentary rocks

One hundred zircons were analysed from the sedimentary and metasedimentary rocks to obtain the detrital zircon age spectra. Greenland Group greywacke (Fig. 1) is characterized by two major peaks at 600–500 Ma, and 1200–1000 Ma, with a smaller peak evident at *c.* 1600 Ma, and individual grains have ages up to *c.* 3500 Ma (Fig. 4a,b). The maximum sedimentary age for the Greenland Group, as given by the cuto in the youngest zircons, is Lower Palaeozoic (*c.* 500 Ma) which is consistent with the Ordovician depositional age (Cooper, 1989). These age patterns are remarkably similar to patterns obtained from the Lachlan Fold Belt of southeastern Australia (Fig. 4c),

Table 2. Monazite U–Th–Pb data for Buckland and Dunphy granites.

Labels	Th/U	f_{206} (%)	f_{208} (%)	$^{208}Pb/^{206}Pb$	$^{208}Pb/^{232}Th$	$^{207}Pb/^{206}Pb$	$^{238}U/^{206}Pb$	Age $^{208}Pb^*/^{232}Th$	Age $^{206}Pb^*/^{238}U$
Buckland Granite									
1.1	56.7±8.0	1.70	0.20	17.531±0.143	0.00539±0.00012	0.0617±0.0013	55.14±1.28	111.2±2.5	113.9±2.6
1.2	64.3±10.8	2.36	0.25	19.662±0.209	0.00543±0.00012	0.0670±0.0017	58.37±1.39	112.0±2.3	106.9±2.5
2.1	13.2±1.5	1.07	0.49	4.525±0.039	0.00551±0.00012	0.0568±0.0012	56.15±1.17	113.3±2.5	112.6±2.3
2.2	20.3±3.9	2.37	0.77	6.376±0.050	0.00536±0.00012	0.0670±0.0035	61.58±1.63	110.0±2.3	101.4±2.7•
3.1	8.5±0.3	0.47	0.37	2.683±0.011	0.00519±0.00012	0.0519±0.0005	60.16±1.43	107.1±2.4	105.8±2.5
3.2	4.5±0.1	0.37	0.56	1.391±0.007	0.00543±0.00011	0.0512±0.0004	59.44±1.27	111.7±2.3	107.2±2.3
4.1	5.8±0.1	0.48	0.54	1.868±0.006	0.00557±0.00012	0.0522±0.0004	56.26±1.19	114.7±2.4	113.0±2.4
4.2	6.6±0.2	0.39	0.40	2.044±0.010	0.00548±0.00012	0.0514±0.0005	58.63±1.20	112.8±2.4	108.6±2.2
5.1	10.4±0.1	0.53	0.33	3.335±0.015	0.00536±0.00011	0.0524±0.0013	56.37±1.17	110.4±2.2	112.8±2.3
5.2	8.8±0.2	0.47	0.36	2.728±0.015	0.00536±0.00012	0.0520±0.0014	58.48±1.21	110.5±2.3	108.8±2.2
6.1	38.0±3.2	1.83	0.32	11.971±0.208	0.00548±0.00011	0.0628±0.0012	55.11±1.24	112.9±2.3	113.8±2.5
6.2	33.3±2.2	1.40	0.29	9.950±0.078	0.00553±0.00012	0.0594±0.0011	55.94±1.55	113.9±2.3	112.6±3.1
7.1	13.8±1.0	0.43	0.21	4.261±0.021	0.00522±0.00011	0.0516±0.0006	58.40±1.22	107.9±2.2	109.0±2.3
7.2	12.7±0.2	0.73	0.39	3.906±0.023	0.00555±0.00012	0.0541±0.0007	57.66±1.20	114.2±2.4	110.0±2.3
8.1	9.5±1.0	0.50	0.34	3.000±0.014	0.00528±0.00012	0.0521±0.0006	58.22±1.21	108.8±2.3	109.2±2.3
8.2	12.1±0.5	1.03	0.56	3.765±0.024	0.00546±0.00012	0.0564±0.0008	59.70±1.26	112.2±2.5	106.0±2.2
9.1	18.7±4.8	0.93	0.33	5.750±0.034	0.00518±0.00011	0.0555±0.0008	59.79±1.28	107.0±2.2	105.9±2.3
9.2	38.1±5.9	2.02	0.36	11.589±0.093	0.00589±0.00012	0.0644±0.0012	54.42±1.46	121.2±2.5•	115.0±3.1
10.1	15.2±0.4	1.33	0.59	4.659±0.047	0.00550±0.00012	0.0588±0.0015	55.00±1.34	113.0±2.4	114.6±2.8
10.2	14.8±0.4	1.51	0.71	4.449±0.033	0.00528±0.00011	0.0602±0.0010	58.34±1.25	108.4±2.2	107.9±2.3
				$^{208}Pb/^{232}Th$ Age			$^{206}Pb/^{238}U$ Age		
Weighted Mean:				(n=19/20; MSWD=1.08) 111.1±0.5 (1σ)			(n=19/20; MSWD=1.62) 109.9±0.6 (1σ)		
Error in standard:				0.44% (1σ)			0.55% (1σ)		
Final age:				111.1±1.5 Ma (2σ)			109.9±1.6 Ma (2σ)		
Dunphy Granite									
1.1	9.9±0.6	0.36	0.24	3.121±0.008	0.0198±0.0007	0.0570±0.0010	16.26±0.57	395.1±13.2	383.5±13.1
1.2	6.4±0.4	0.41	0.43	1.997±0.012	0.0198±0.0007	0.0574±0.0008	16.45±0.52	394.4±12.9	379.0±11.8
2.1	8.4±0.7	0.18	0.14	2.675±0.049	0.0218±0.0020	0.0555±0.0003	15.38±0.90	435.3±41.5	405.3±23.0
2.2	8.4±0.1	0.26	0.20	2.669±0.006	0.0193±0.0006	0.0562±0.0005	16.86±0.51	384.8±12.2	370.5±10.9
3.1	11.4±0.4	0.39	0.22	3.655±0.009	0.0190±0.0006	0.0572±0.0006	16.96±0.54	378.9±11.5	368.0±11.5
4.1	8.5±0.4	0.21	0.16	2.696±0.011	0.0188±0.0006	0.0558±0.0003	16.96±0.54	375.6±11.7	368.5±11.5
5.1	8.1±0.2	0.16	0.13	2.532±0.009	0.0190±0.0006	0.0554±0.0004	16.64±0.52	380.2±11.6	375.6±11.4
6.1	2.1±0.1	0.28	0.98	0.605±0.006	0.0186±0.0006	0.0564±0.0003	16.65±0.55	369.2± 11.3	375.0±12.1
7.1	4.9±0.2	−0.06	−0.08	1.512±0.007	0.0185±0.0006	0.0536±0.0009	16.96±0.52	370.9±11.3	369.5±11.1
8.1	10.7±0.6	−0.22	−0.14	3.395±0.008	0.0190±0.0006	0.0523±0.0006	16.22±0.51	380.7±11.8	386.4±11.8
8.2	6.9±0.2	−0.05	−0.05	2.147±0.005	0.0180±0.0005	0.0537±0.0002	17.55±0.53	360.4±11.1	357.5±10.6
9.1	7.4±0.2	−0.19	−0.17	2.349±0.005	0.0188±0.0006	0.0526±0.0009	17.01±0.53	377.2±11.4	368.9±11.2
9.2	8.9±0.4	−0.14	−0.18	1.714±0.485	0.0117±0.0030	0.0529±0.0007	17.71±0.55	235.6±62.4•	354.5±10.8
11.1	8.9±0.5	0.37	0.26	2.957±0.017	0.0193±0.0006	0.0571±0.0003	16.62±0.54	385.0±13.0	375.3±11.9
3.2	8.0±0.4	0.48	0.38	2.649±0.018	0.0182±0.0043	0.0580±0.0007	18.12±0.56	363.9±88.0	344.6±10.4
10.1	9.4±0.4	0.42	0.27	3.189±0.007	0.0186±0.0006	0.0574±0.0003	17.41±0.55	372.0±12.1	358.5±10.9
13.1	8.3±0.3	0.49	0.59	1.730±0.470	0.0120±0.0031	0.0580±0.0008	16.72±0.61	240.2±63.8•	372.6±13.3
14.1	9.5±0.4	1.71	1.13	3.167±0.007	0.0189±0.0006	0.0679±0.0003	17.09±0.54	374.1±11.3	360.4±11.1
15.1	6.4±0.1	0.33	0.33	2.128±0.008	0.0184±0.0006	0.0568±0.0006	17.25±0.59	366.5±11.6	362.1±12.1
				$^{208}Pb/^{232}Th$ Age			$^{206}Pb/^{238}U$ Age		
Weighted Mean:				(n=17/19; MSWD=0.67) 377.2±3.0 (1σ)			(n=19/19; MSWD=0.99) 368.0±2.7 (1σ)		
Error in standard:				0.73% (1σ)			0.76% (1σ)		
Final age:				377.2±8.0 Ma (2σ)			368.0±7.6 Ma (2σ)		

Errors are 1σ unless otherwise stated.
• Denotes outlier from weighted mean age.

which suggests original contiguity of the Western Province of New Zealand with southeastern Australia.

The two paragneisses from Westland (Fig. 5) and the schists from Fiordland (Fig. 6) share the same detrital zircon pattern, which is identical in style to that of the Greenland Group greywacke. From this it is clear that the Greenland Group is a suitable source for the paragneisses on the West Coast, as proposed by Laird (1967) and as suggested by whole-rock Nd-isotope characteristics (Pickett & Wasserburg, 1989). Furthermore, this detrital zircon pattern is also found in sillimanite-grade paragneisses in Fiordland (Gibson & Ireland, 1996) and it is thus possible that Greenland Group is the protolith for these paragneisses as well. However, it should be noted, that Delamarian sedimentary units such as the Kanmantoo Group of South Australia also share this pattern (Ireland *et al.*, 1995; Gibson & Ireland, 1996), and so the sedimentary pattern itself may not be uniquely diagnostic of a particular source terrane on the Gondwana margin.

Charleston orthogneiss

Zircon. As suggested from the conventional analysis of this zircon fraction (Kimbrough & Tulloch, 1989), the zircons show a range of ages (Fig. 7a). These ages are shown by individual crystals and also as core/rims and other structural inclusions of individual zircons. Some single zircons have up to three distinct age components

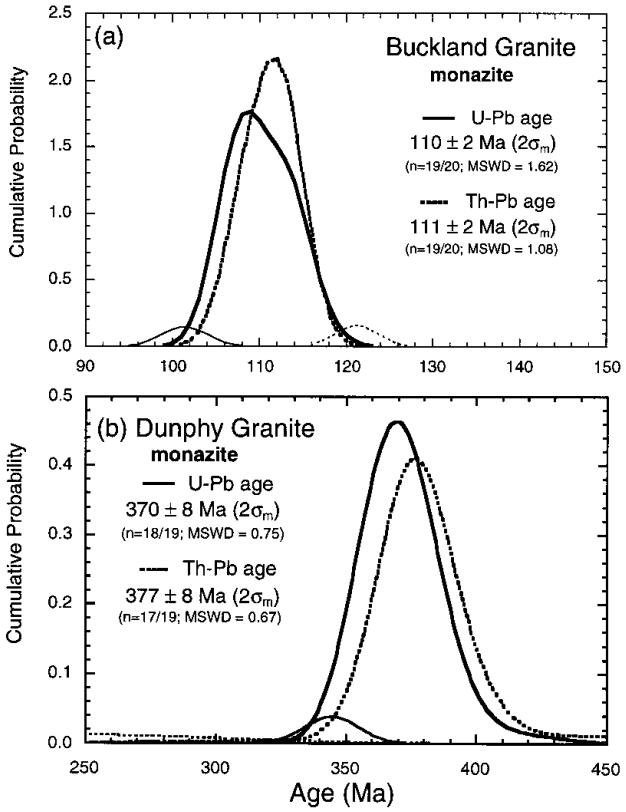

Fig. 3. Cumulative-probability age diagrams for monazites from Buckland Granite and Dunphy Granite. (a) One outlier from each of the U–Pb and Th–Pb sets have been removed. Outliers are plotted as the narrower line gaussians to the lower (U–Pb) and higher (Th–Pb) sides of the main peaks. Both monazite ages agree well with the ion-probe zircon age of this rock, which is 109.6 ± 1.7 Ma (Muir *et al.*, 1994). (b) Two low-precision Th–Pb ages have been excluded from the final age calculation. The monazite ages agree well with the zircon age of this rock, which is 377.8 ± 4.5 Ma (Muir *et al.*, 1996a), although both monazite ages are on the lower side of the zircon U–Pb age.

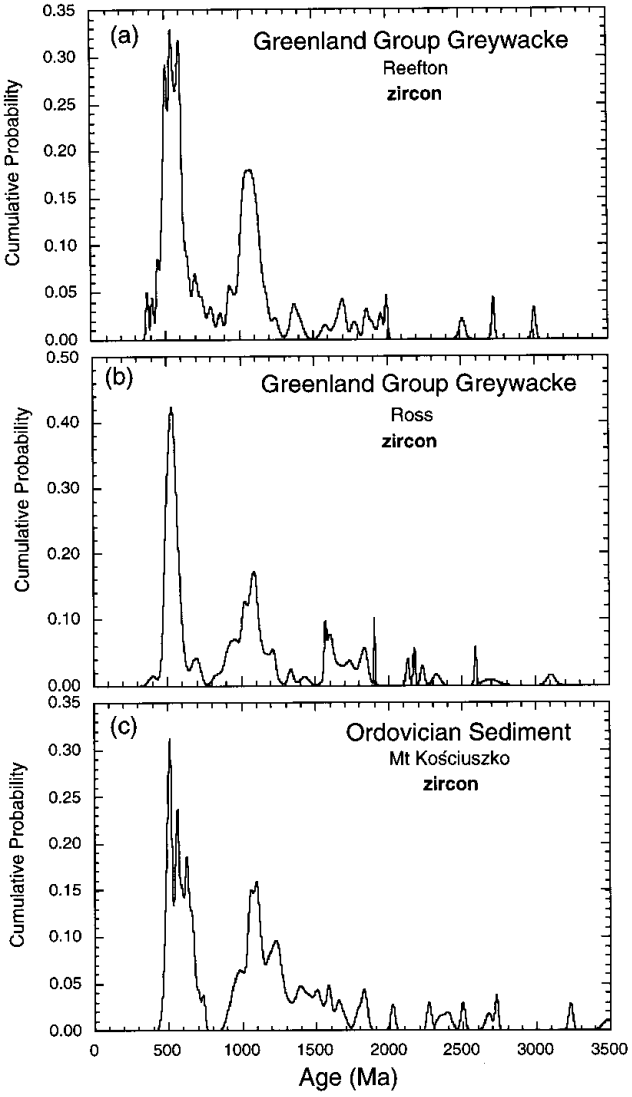

Fig. 4. Detrital-zircon cumulative-probability age diagrams of (Ordovician) Greenland Group greywackes from (a) Globe Mine, near Reefton, and (b) Totara River near Ross. The histogram in (c) is from an Ordovician sediment on the eastern side of Mt Kosciuszko, Australia. The similarity between the New Zealand and Australian sedimentary rocks suggests the original contiguity of the sedimentary sequence.

(e.g. *c.* 900 Ma core, massive *c.* 360 Ma rim and a thinner *c.* 120 Ma rim). The ages represented in the orthogneiss are broadly the same as those represented in the Westland sediments and intrusive rocks. That is, 500 Ma and older zircons are consistent with derivation from Greenland Group greywacke, *c.* 370–330 Ma zircons are consistent with derivation from Karamea intrusive rocks, and *c.* 120–110 Ma ages are consistent with the Separation Point and Rahu intrusive rocks. However, the abundances cannot be separated into particular protoliths so readily, because the Karamea Granite contains significant Greenland inheritance, as do Rahu suite intrusions like the Buckland Granite. In fact, the Buckland Granite shows nearly all the age components represented in the orthogneiss, the main di erences being in the abundances of the components. However, a small component of zircon with an age of *c.* 250 Ma in the orthogneiss is not represented in any Western Province granites dated so far; this zircon age is more typically found in the Eastern Province, such as in the Torlesse terrane (Ireland, 1992).

The Cretaceous ages around 120–110 Ma show more scatter than would be predicted for a single peak. Deconvolving the peak gives a satisfactory solution for two components: the main peak at 119 Ma and a smaller peak at 109 Ma (Fig. 7b). It is probably no coincidence that these two ages reflect the intrusion of the Separation Point Suite and Rahu Suite intrusives, respectively. The relatively small size of the 109 Ma peak suggests that the orthogneiss derives, in large part, from metamorphism of a SPB protolith brought about by emplacement of the Buckland Granite.

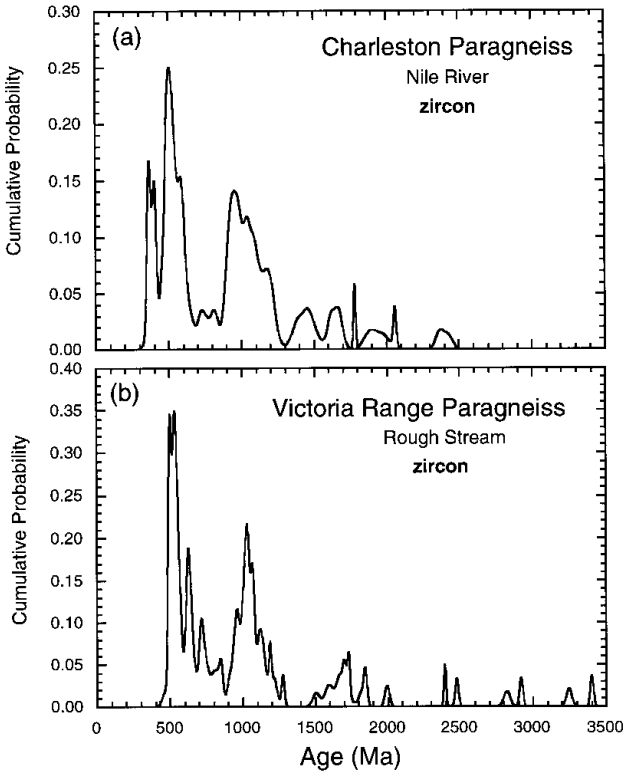

Fig. 5. Zircon-age histograms of paragneisses from the Nile River mouth, Charleston, and from Victoria Range. The general similarity between these spectra and those from the Greenland Group greywackes suggests that the greywackes are the protoliths for the Westland paragneisses.

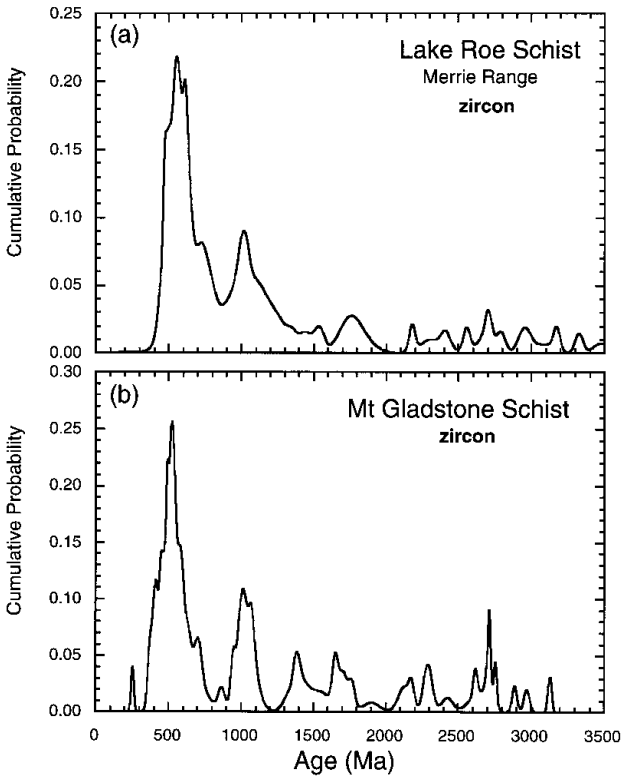

Fig. 6. Zircon-age histograms of (a) Lake Roe (sillimanite-bearing) schist and (b) Mt Gladstone (kyanite-bearing) schist. These patterns are similar to the Greenland Group greywacke, indicating that Lower Palaeozoic sedimentary rocks such as the Greenland Group are suitable protoliths for these schists. However, some Delamarian sedimentary rocks have also been found with this detrital pattern (Gibson & Ireland, 1996) and so a definitive association cannot be made on detrital zircon patterns alone.

Monazite. Th/U in these monazites ranges from 9.6 to 19.2 and the fraction of common Pb ranges up to 3.2% for f^{206}Pb, the fraction of common ^{206}Pb to total ^{206}Pb, and 1.8% for f^{208}Pb. A cumulative-probability plot for monazites analysed from Charleston orthogneiss (90–428) is shown in Fig. 8. One clear outlier in the U–Pb data has a large error; this datum is not an outlier in the Th–Pb system and its large U–Pb error is due to an analytical e ect. The first two Th–Pb measurements were compromised by misalignment of the Th field position that was rectified after the first two analyses; these are not included in the Th–Pb data set, but the U–Pb measurements are included. The U–Pb 111 ± 2 Ma ($2\sigma_m$; MSWD = 1.02) and Th–Pb (112 ± 2 Ma; MSWD = 0.70) ages agree within error. This age is consistent with the lower concordia intercept zircon age (118 ± 14 Ma) of Kimbrough & Tulloch (1989) and also the youngest zircon peak determined by ion probe (Fig. 7b).

Charleston paragneiss/Victoria Range paragneiss

Monazite. Monazite separated from the Charleston paragneiss is identical in shape and size characteristics to the Charleston orthogneiss. Very little monazite was found in the Victoria Range paragneiss sample and only 14 small monazites were mounted for ion probe analysis.

For the Charleston paragneiss monazite, Th/U ranges from 7.6 to 13.8 and the fraction of common Pb is under 1% for all data from both systems. One outlier is rejected from each of the U–Pb and Th–Pb sets. Both outliers are younger than the mean, suggesting Pb loss is the cause. The mean U–Pb (361 ± 6 Ma (2σ); MSWD = 0.96) and Th–Pb (367 ± 6 Ma; MSWD = 1.48) ages agree within error (Fig. 9a). For the Victoria Range paragneiss monazite, Th/U ranges from 4.2 to 8.8 and the fraction of common Pb is under 1% for all analyses except 12, the U–Pb age of which is the sole outlier in this data set (although one analysis (10) was rejected for analytical unreliability). The U–Pb outlier is on the young side of the mean, suggesting Pb loss as a possible cause. The mean U–Pb (377 ± 7 Ma ($2\sigma_m$); MSWD = 1.75) and Th–Pb (374 ± 7 Ma; MSWD = 1.05) ages agree within error (Fig. 9b). Despite the di erent morphological characteristics, monazites from the two paragneisses give very similar ages and, more

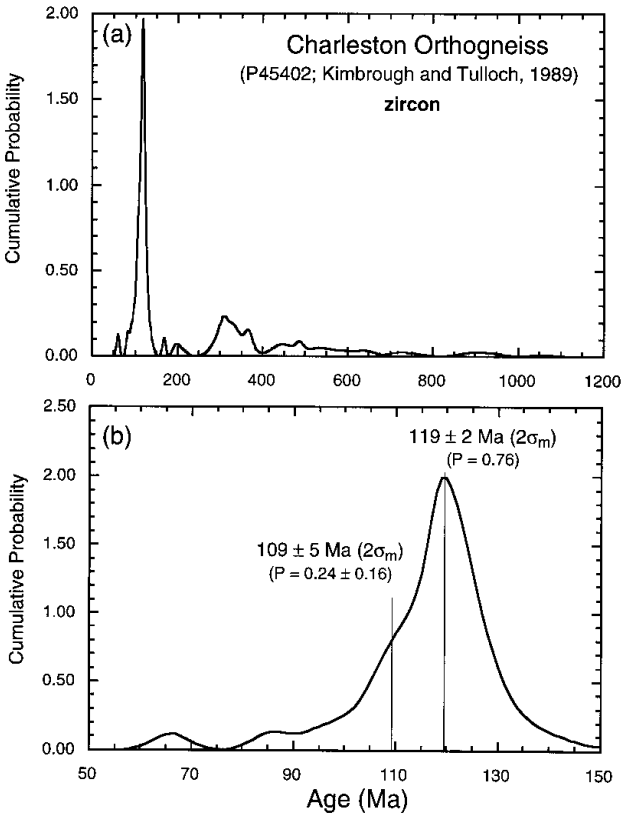

Fig. 7. (a) Zircon-age histogram of Charleston orthogneiss P45402 (Kimbrough & Tulloch, 1989), showing a strong Cretaceous peak as well as inherited granite (300–380 Ma) and sedimentary (*c.* 500 and older) components. (b) A cumulative-frequency plot of the Cretaceous peak shows two components, one at 119 Ma and a smaller peak at 109 Ma. The 119 Ma age is typical of Separation Point Suite, whereas 109 Ma is typical of Rahu Suite granites. Mixture modelling (Sambridge & Compston, 1994) yields the ages and uncertainties indicated. The proportions (P) of each peak are also indicated, with the uncertainty attributed to the smaller peak.

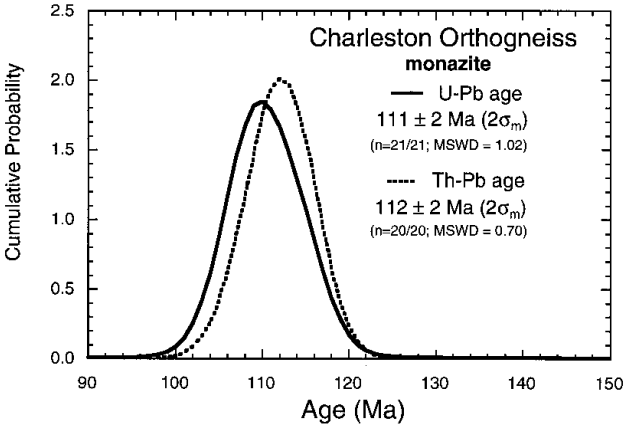

Fig. 8. Cumulative-probability diagrams for monazite data from Charleston orthogneiss. Despite the mixed parentage of this rock as evidenced from the zircons in Fig. 7a, the monazites show a single age, which is similar to that for the Buckland Granite and the youngest zircon peak in Fig. 7b.

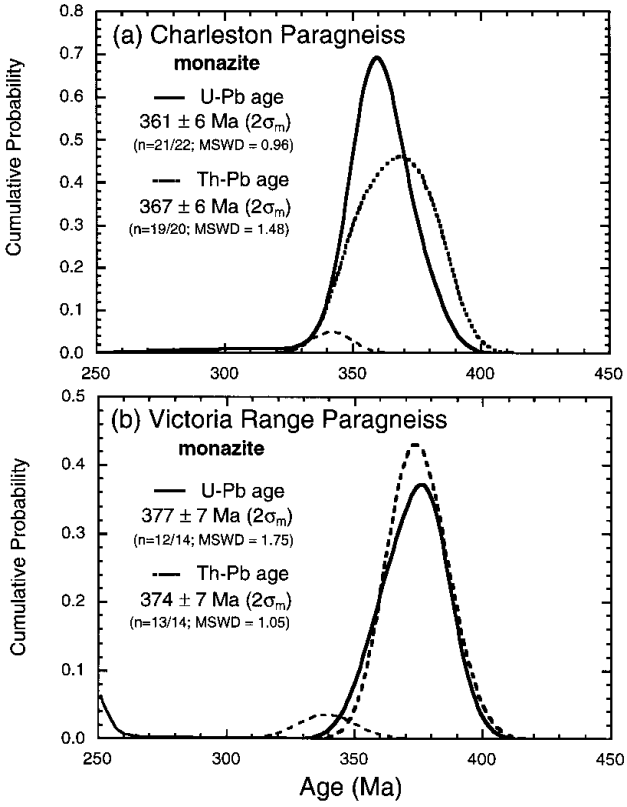

Fig. 9. Cumulative-probability diagrams for monazite data from (a) Charleston paragneiss and (b) Victoria Range paragneiss. One young U–Pb analysis (o -scale) from the Charleston paragneiss has been excluded, as has one young Th–Pb analysis. Two young U–Pb and one young Th–Pb ages have been excluded in calculating the mean age for the Mt Victoria paragneiss. The ages of monazites from these paragneisses are consistent with metamorphism following emplacement of the granites of the Karamea Batholith.

important, point to a Devonian rather than Cretaceous or Precambrian age of metamorphism.

Lake Roe schist (M1 – sillimanite grade)

Monazite. The monazite grains analysed from this rock do not all belong to a single population. A cumulative probability plot of the 25 analyses of individual monazite grains shows a range in age from around 350 to over 1000 Ma (Fig. 10a). Distinct peaks are present at *c.* 350 Ma, and 500 Ma with a few older grains; a single grain has a U–Pb age of *c.* 1050 Ma. Attempting to constrain the youngest peak requires the deconvolving of the older material away from ages that are consistent with the main peak. The youngest nine U–Pb analyses give a weighted mean U–Pb age of 356 ± 9 Ma (MSWD = 1.13) (Fig. 10b) and the youngest seven Th–Pb ages give a weighted mean age of 368 ± 8 Ma (MSWD = 0.63). In general, there is a good correspondence between the U–Pb and Th–Pb ages, but some exceptions are noteworthy: for example,

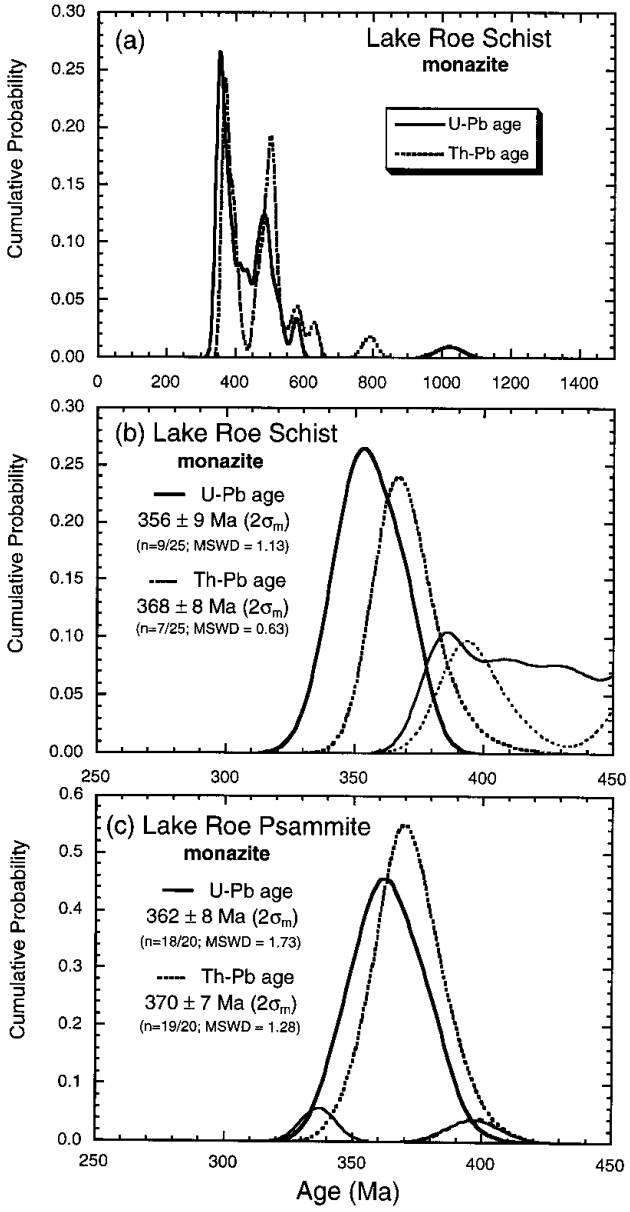

Fig. 10. Cumulative-probability diagrams for monazite data from Lake Roe pelitic schist (a,b) and psammite (c). (a) Ages from this rock range from around 360 Ma up to 1000 Ma. Detrital monazites are preserved in this schist, as evidenced by the similarity in the older monazite ages with the main peaks in the zircon age distribution (Fig. 6a). (b) Expanded view of the younger U–Pb and Th–Pb peaks indicating metamorphic monazite ages. (c) The Lake Roe metapsammite monazite data and the U–Pb and Th–Pb ages agree within error at around 360 Ma, and agree with the youngest peak in the Lake Roe pelitic schist. This age is interpreted as representing the sillimanite (M1) metamorphic event in the Tuhua sequence.

grain 10 has a 460 Ma Th–Pb age and a 370 Ma U–Pb age.

If the youngest peak is interpreted as the metamorphic age, the inheritance bears a strong resemblance to the detrital zircon pattern from Greenland Group greywacke. This is also consistent with the di ering U–Pb and Th–Pb ages from some grains, i.e. the U–Pb and Th–Pb systems have been reset to di erent degrees, but does not preclude growth of new monazite during metamorphism either. Morphologically, it is not possible to distinguish between metamorphic and inherited monazite and there is no distinction in the range of Th/U for these grains. One distinguishing characteristic of this sample is that a much larger amount of monazite was separated than for any other sample.

In prograde metamorphism, it has been found that detrital monazite is unstable in metapelitic assemblages at greenschist facies conditions, breaking down to REE and Th oxide grains before becoming stable again in upper-amphibolite facies rocks (Smith & Barreiro, 1990; Kingsbury *et al.*, 1993). However, the Lake Roe schist monazites show a wide range of ages, which are best interpreted in terms of pre-existing (detrital) monazite. Monazite inheritance is rare and the best examples come from leucogranites from the Himalayas (Copeland *et al.*, 1988; Harrison *et al.*, 1995). Thus, monazite can apparently survive the thermal resetting of granite formation, and it is the chemistry of metapelites that causes monazite to break down (Kingsbury *et al.*, 1993). Watt & Harley (1993) and Watt (1995) have also found that monazite can survive disequilibrium melting in the dry conditions of high-grade peraluminous metapelites.

Lake Roe psammite (M1 – sillimanite grade)

Monazite. Th/U ratios range from 8 to 16 and f^{206}Pb is less than 0.1% in all analyses. The U–Pb analyses form a single peak, although the MSWD is excessive at 2.9. One point lies 3.4σ below the mean, the other 3.5σ above; rejecting these points gives a mean U–Pb age of 362 ± 8 Ma with a MSWD of 1.73 (Fig. 10c). One Th–Pb age is marginally high (2.7σ) and, if this point is rejected, a mean of 370 ± 7 Ma is obtained with a MSWD of 1.28. The U–Pb and Th–Pb ages agree with each other and are also consistent with the age obtained from the youngest peak of the Lake Roe schist (Fig. 10b).

Mt Gladstone schist (M2 – kyanite grade)

Monazite. Only 10 small grains of monazite were recovered and mounted. Replicate analyses were made on these 10 grains after repolishing the mount to remove the pits generated in the first session of analyses. Th/U ratios for these grains are generally in the range of 12–50 and the common ^{206}Pb fraction is less than 1% in all grains. The 20 analyses of these 10 grains are well clustered (Fig. 11a), although there is excess scatter in both U–Pb and Th–Pb systems. The 20 U–Pb analyses give a MSWD of 2.4, and rejecting the two lowest values gives a satisfactory MSWD of 1.63 and a mean age of 328 ± 5 Ma ($2\sigma_m$). The 20 Th–Pb analyses give a MSWD of 2.1. The most

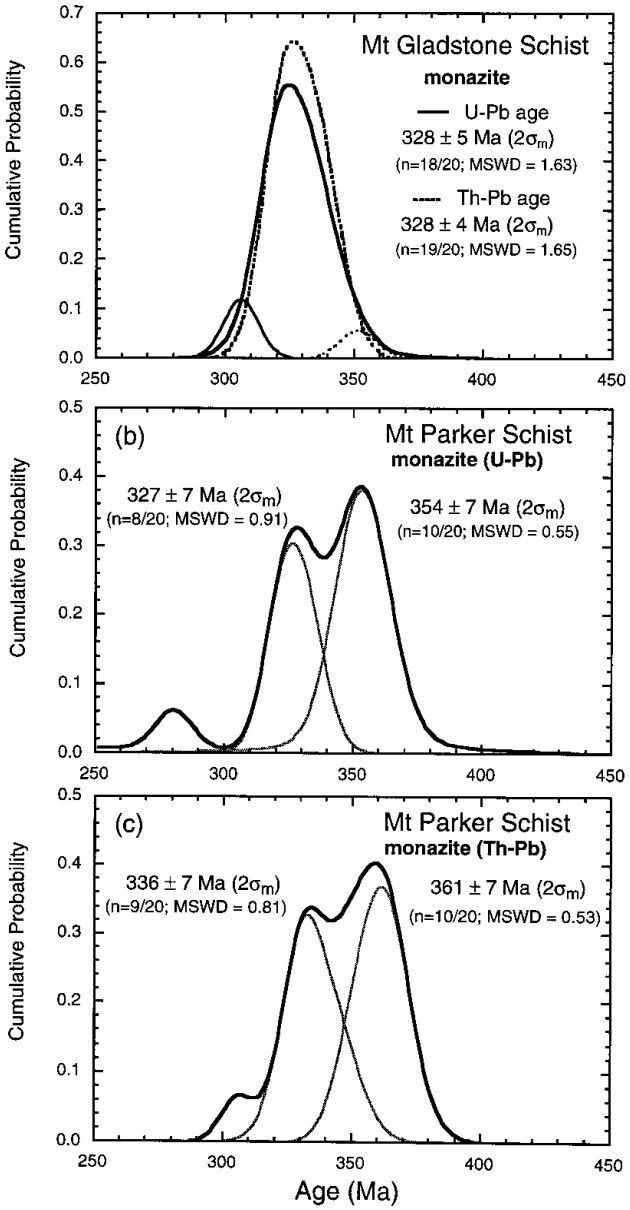

Fig. 11. Cumulative-probability diagrams for monazites from (a) Mt Gladstone schist and (b,c) Mt Parker schist. (a) The data are consistent with a single group, albeit with two young outliers from the U–Pb data and one older outlier from the Th–Pb data. The Th–Pb age and the U–Pb ages agree within error at 330 Ma, which we take as the M2 metamorphic age, some 30 Ma younger than the M1 metamorphism. (b,c) Like the Mt Gladstone schist, the Mt Parker schist has experienced the M2 event, but both U–Pb and Th–Pb age spectra reveal bimodality. The deconvolved ages are consistent with the older *c.* 360 Ma peaks being an inherited component from the M1 event whereas the younger peaks are consistent with the 330 Ma M2 age determined from the Mt Gladstone schist.

removed outlier is high and its rejection gives a satisfactory MSWD of 1.65 and a mean Th–Pb age of 328 ± 4 Ma. The U–Pb and Th–Pb ages agree within error.

Mt Parker schist (M2 – kyanite grade)

Monazite. Twenty Mt Parker monazite grains give Th/U ratios ranging between nine and 21 and the common ^{206}Pb fraction is less than 1% in all grains. The 20 U–Pb analyses give a MSWD of 6.9 and the Th–Pb analyses 4.8. After rejecting analysis four, which is low in both U–Pb and Th–Pb systems by greater than 6σ respectively, the MSWD falls to 3.6 for U–Pb, and 2.9 for Th–Pb. The remaining data form bimodal distributions in both U–Pb (Fig. 11b) and Th–Pb (Fig. 11c) systems. These two peaks were deconvolved by spectral deconvolution (Sambridge & Compston, 1994), which produces a non-subjective splitting of the peaks. The analyses were also deconvolved by examining the probability density function of the U–Pb and Th–Pb analyses and assigning each peak to older or younger on the basis of the combined U–Pb and Th–Pb age. There is no di erence in the ages calculated for the peaks by either method. The ages of the U–Pb peaks are 327 ± 7 Ma and 354 ± 7 Ma and the Th–Pb ages are 336 ± 7 Ma and 361 ± 7 Ma ($2\sigma_m$).

Therefore, the Mt Parker schist appears to contain two populations of monazite, although no morphological or chemical distinction can be found between the two age groups. The older of these age groups at around 360 Ma is the same as that for M1 metamorphism, as given by the youngest peak of Lake Roe schist (Fig. 10b) and the mean age for the Lake Roe metapsammite (Fig. 10c). The younger peak at 330 Ma agrees in age with the Mt Gladstone schist, which dates the M2 metamorphism. Thus, it appears that the Mt Parker schist preserves a component from the earlier M1 metamorphism and this survived M2 metamorphism, when either new monazite was formed or a fraction of the existing M1 monazite was reset. Given the separation of the peaks in Fig. 11b,c, it is likely that new monazite has formed without disturbing pre-existing M1 monazite; otherwise a continuum of ages between 360 and 330 Ma would be expected.

Orthogneiss intrusives in kyanite schists

Zircon. Gibson & Ireland (1996) presented zircon U–Pb data from a strongly deformed granitic rock (95-301), which has an age of 334.6 Ma $\pm$ 5.2 Ma. This granite is hosted by kyanite-grade pelitic schist and underwent metamorphism contemporaneously with the latter. Also a ected by kyanite grade metamorphism is a discordant granite orthogneiss (95-300). Zircon analyses from both of these samples are plotted in a cumulative frequency diagram in Fig. 12. The U–Pb characteristics of these two samples are very similar. Pb loss is apparent, with a cluster of young analyses on the young side of the main peaks. In sample 95-300, only one clear outlier is apparent. The MSWD of the remaining 14 samples is 1.8, which is

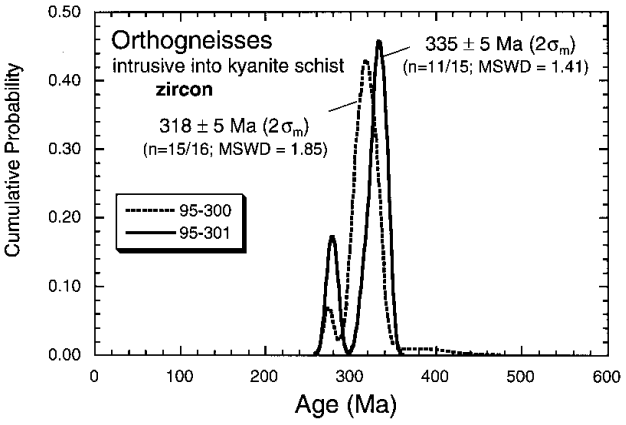

Fig. 12. Cumulative-probability diagram for orthogneisses in kyanite-grade schist. Data from sample 95-301 was reported in Gibson & Ireland (1996). Orthogneiss 95-300 is slightly younger than 95-301, but both orthogneisses are similar in age to monazite from the host kyanite grade schists.

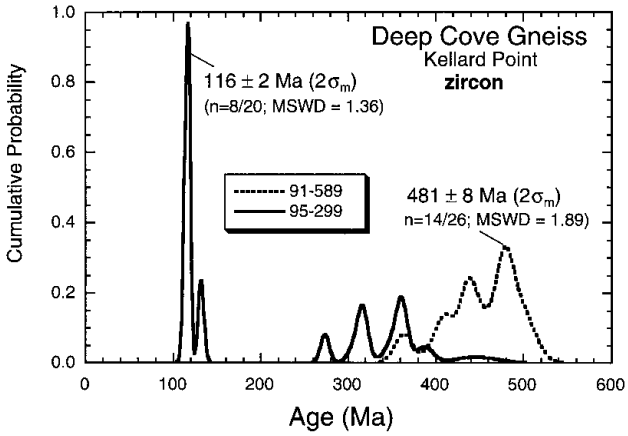

Fig. 13. Cumulative-probability diagrams for Deep Cove Gneiss samples. Data from sample 91-589 was reported by Gibson & Ireland (1996) and indicates Cambro-Ordovician granites are present in Fiordland. Of more concern here is the presence of Cretaceous zircon in Deep Cove Gneiss sample, 95-299. The zircon chemistry suggests that new metamorphic zircon has grown in the Cretaceous as a result of heating associated with late Mesozoic thermal activity.

marginally higher than that expected from analytical uncertainty alone. The mean age of these analyses is 318 ± 5 Ma ($2\sigma_m$). This age is lower than the 335 ± 5 Ma determined for 95-301 and is consistent with the discordant nature of 95-300. Nevertheless, both of these samples lie within the age range of monazites from the kyanite schists.

Deep Cove Gneiss

Zircon. Gibson & Ireland (1996) analysed a sample of orthogneiss from Deep Cove Gneiss (91-589) that gives an inferred age of *c.* 480 Ma. We analysed another sample of Deep Cove Gneiss (95-299) in an attempt to further constrain the emplacement age of this rock. The results have the added advantage of illustrating some of the problems in determining accurate ages from the high-grade gneisses in Fiordland. Although a Palaeozoic component is present, eight of the 15 zircon analyses lie within error of an age of 116 ± 2 Ma ($2\sigma_m$) (Fig. 13). These zircons all have high U (≥ 1000 p.p.m.) and low Th/U (<0.4) whereas the older zircons have generally lower U and more variable Th/U (0.4–1.4). The former are consistent with growth of new metamorphic zircon at *c.* 116 Ma and yield a markedly younger age than zircons from other samples of orthogneiss in Deep Cove Gneiss, such as 91-589. If sample 95-299 were considered on its own, it would be di cult to decide whether this is a Palaeozoic granite with Cretaceous Pb loss/new growth or whether this is a Cretaceous granite with Palaeozoic inheritance. However, given that the host orthogneiss (sample 91-589) does not have a Cretaceous component, we conclude that sample 95-299 is a Palaeozoic granite which has experienced a strong thermal event in the Cretaceous.

THERMOBAROMETRY

Westland

Thermobarometry of paragneisses in the Paparoa Range of Westland (Fig. 1) has been reported previously (White, 1994). He concluded that the gneisses experienced a single major metamorphic event; mineral assemblages indicate upper-amphibolite facies metamorphism. The presence of a K-feldspar–sillimanite isograd, together with thermobarometry on coexisting minerals, indicate a temperature range of 600–700 °C and pressure of 4 ± 1 kbar with very little variation throughout the region.

At Charleston, the presence of sillimanite–garnet assemblages (without cordierite) in the paragneisses has been taken by Kimbrough & Tulloch (1989) to indicate that peak temperatures of around 540–700 °C and pressures in excess of 4–5 kbar were attained.

Fiordland

The thermobarometry of the Fiordland rocks is complicated by the overprinting associated with the three deformational events recognised. Sillimanite-grade rocks (M1 metamorphism) contain little or no garnet and thermobarometric data are available for only two samples (Otago University samples 41151 and 40887). These rocks formed under a steeper thermal gradient (60–65 °C km^{-1}) than their kyanite-bearing counterparts and give temperatures (630–680 °C) and pressures (3–6 kbar) consistent with metamorphism in a low-*P*/high-*T* environment (Gibson *et al.*, 1988; Gibson, 1992). Low-*P*/high-*T* metamorphism is also supported by the occurrence of cordierite

in metapelitic assemblages and the widespread development of migmatites. Many sillimanite-bearing metapelitic rocks also contain K-feldspar rather than muscovite, indicating that temperatures during M1 exceeded the stability limits of muscovite. For the pressures cited here, temperatures above 600–650 °C are indicated. A second, much younger generation of fibrous sillimanite (syn- to post-D3) formed during late Mesozoic decompression; it is petrographically distinct from the coarser grained M1 sillimanite that defines the D2 schistosity (S2) and commonly forms veinlets that cut S2.

Temperatures calculated for M2 kyanite-grade assemblages range from 580–780 °C. Pressures increase from 5 kbar in central Fiordland to 9 kbar farther west, where the deepest structural levels are preserved. Sillimanite, if it is present at all in these assemblages, typically persists only as inclusions in garnet, whereas kyanite occurs both within the matrix and as inclusions in garnet rims. Moreover, in several instances, these sillimanite inclusions define an earlier foliation (S1) which is no longer preserved in the matrix. Furthermore, S1 is commonly oriented at high angles to S2. Kyanite metamorphism overprints and post-dates the first-generation sillimanite assemblages and points to an episode of crustal thickening subsequent to the earlier M1 low-P/high-T event.

Formation of M2 assemblages during, or immediately following crustal thickening is also supported by compositional profiles through garnet, showing increasing grossular component from core to rim (Bradshaw, 1989; Gibson, 1990; Brown, 1996). Concomitant with this increase of grossular component in garnet, plagioclase grains become more sodic towards their rims. Garnet growth evidently occurred through a reaction involving the simultaneous breakdown of the anorthite component in plagioclase (Gibson, 1979; 1990; Bradshaw, 1989; 1990). This particular reaction also produces aluminosilicate and quartz, and being pressure sensitive, has long been recognized as a useful geobarometer (Ghent & Stout, 1981; Newton & Haselton, 1981).

DISCUSSION

Westland/Northwest Nelson

The age of orthogneiss from Charleston has remained somewhat equivocal, despite the U–Pb zircon measurements of Kimbrough & Tulloch (1989). In large part of this is due to the di culties of interpreting zircon U–Pb systematics, which indicate the preservation of older age components. Kimbrough & Tulloch (1989) interpreted their lower intercept age of 114 ± 18 Ma as the intrusion age of orthogneiss protoliths around Charleston. Despite the large error on the lower intercept and the high MSWD (1380), some confidence can be placed in the Cretaceous age because of the clustering of the data towards the lower intercept. In contrast, the 680 ± 21 Ma Rb–Sr isochron ($n = 5$; MSWD = 2.1) of Adams (1975) is a clear illustration of a good statistical solution being geologically meaningless (q.v. Kimbrough & Tulloch, 1989). Isochrons such as this may give a geologically realistic age, but it is almost impossible to judge the veracity of interpretations without further independent geochronological and geological data.

From the ion microprobe data presented in Fig. 8a, it can be seen that Cretaceous zircons dominate. Moreover, the ion microprobe zircon data reveal two components in the Cretaceous peak: the dominant peak at 119 Ma, and a smaller peak at 109 Ma, which lies within error of the monazite U–Pb and Th–Pb ages. These data accurately and precisely establish the age of metamorphism and tectonism of the Charleston orthogneiss at 110 Ma, with very little room for error towards higher or lower ages. This age is contemporaneous with the Buckland Granite of the Rahu Suite, whereas the older 119 Ma age is typical of Separation Point Suite. Kimbrough & Tulloch (1989) compared the chemistry of Charleston orthogneisses with that of granites from Rahu Suite, Separation Point Suite, and Karamea Suite, and noted the similarity between the Mesozoic intrusives and the orthogneisses. In particular, the high Sr and Ba, low Nb, Zr and Rb, and $K_2O/Na_2O < 1$, are indicative of a large component of Separation Point Suite, consistent with the zircon age populations. Thus, it appears that the orthogneisses were formed from a dominantly Separation Point protolith, metamorphism and tectonism being contemporaneous with the emplacement of the Buckland Granite at 110 Ma.

The metamorphic age of the Westland paragneisses has been largely unconstrained, although putative ages have ranged up to the Precambrian (Tulloch & Kimbrough, 1989; White, 1994). Shelley (1970) proposed that the first deformation of the Charleston gneisses was Tuhuan (mid Palaeozoic), whereas the final deformation was Rangitatan (late Cretaceous), which is the basic chronological scheme determined in this work. Monazite dating shows that the paragneisses were metamorphosed at around 360 Ma, and that these ages are similar to, or only slightly younger than, the zircon age of Karamea batholith granites at 375–370 Ma (Muir *et al.* 1994, 1996a), consistent with thermal metamorphism accompanying and/or following emplacement of the Karamea Batholith.

Overall, the analytical results presented here indicate widespread Devonian metamorphism of the metasedimentary basement. The regional nature of this early metamorphism is further supported by the uniformity of the thermobarometric data in the Paparoa Range (White, 1994). On the other hand, Cretaceous metamorphism associated with the emplacement of Rahu Suite plutons appears to be more localized. In particular, monazite in the paragneisses has not been a ected by orthogneiss emplacement, despite the outcrops being separated by less than 1000 m.

Cretaceous metamorphism thus appears to be limited to the thermal aureoles around intrusions and the more strongly deformed magmatic rocks preserved in the lower plate of the late Mesozoic metamorphic core complexes; it is not pervasively developed on a regional scale.

The Westland gneisses show no evidence for Precambrian continental basement. The paragneisses formed through the metamorphism of Palaeozoic sedimentary rocks, such as the Greenland Group, as evidenced through similar detrital zircon age spectra. Although Precambrian zircons occur in the sedimentary rocks and the gneisses, they are detrital and reflect the presence of old continental basement elsewhere. Furthermore, the oldest granites have no inherited zircons (Gibson & Ireland, 1996). The oldest rocks in New Zealand are Cambro-Ordovician rocks, which were probably deposited on the margin of Gondwana on oceanic crust.

Fiordland

The geochronology of Fiordland has long been dogged by controversy, not least because of uncertainty surrounding the extent to which the Tuhua sequence was a ected by emplacement of the Early Cretaceous WFO. Although many previous workers (e.g. Oliver, 1980; Gibson *et al*., 1988) favoured a mid-Palaeozoic age for the low-*P*/high-*T* metamorphism in this sequence, Bradshaw (1989) and Bradshaw & Kimbrough (1989) argued that the sillimanite-grade metamorphism was due to emplacement of the WFO protolith and that thereafter both the WFO and Tuhua Sequence were subjected to higher pressure, kyanite-grade metamorphism following a continent—continent or continent—island arc collision. Geochronological data presented in this paper indicate that the bulk of the metamorphism in the Tuhua Sequence in west-central Fiordland is of mid-Palaeozoic age. Sillimanite grade (M1) rocks were overprinted *c*. 30 Ma later by a higher pressure kyanite grade event (M2). Given the complexities of Fiordland geology, it is perhaps surprising that more U–Pb analyses have not been found to have been a ected by Cretaceous orogenesis. In part, this reflects our choice of samples. Cretaceous deformation is far from pervasive, with the bulk of strain partitioned into regionally extensive shear zones. Samples showing evidence of Cretaceous deformation were avoided.

Although K–Ar systematics are compromised by Mesozoic partial resetting, the U–Pb system is much less susceptible. Nevertheless, the samples of Deep Cove Gneiss (Fig. 13) reveal the behaviour expected for partial resetting of the U–Pb system by a pervasive Cretaceous thermal event. New zircon formed at 116 Ma and the protolith ages have been variably reset. In contrast, kyanite schists and orthogneisses show no evidence of new monazite growth in the Cretaceous. Furthermore, because both monazite (from the kyanite grade schists) and zircon (from the orthogneiss intrusives) give ages that closely agree at *c*. 330 Ma, partial resetting of Devonian monazite or zircon is not a possible cause for the Carboniferous ages, because monazite and zircon behave di erently in terms of di usive Pb loss. We conclude that kyanite-grade metamorphism is Palaeozoic and cannot be related to the metamorphism in the WFO.

The chronological juxtaposition of high-grade assemblages in Fiordland is remarkably similar to that of the inverted metamorphic sequence beneath the main central thrust of the Himalayas (Harrison *et al*., 1997). In this region metamorphism on the hanging wall has been dated at around 22 Ma (Harrison *et al*., 1995 and references therein) and metamorphism to similar grade in the footwall was assumed to be the same age, because of the present close spatial association. However, ion microprobe monazite dating shows the metamorphism on the footwall to be only 6 Ma and hence unrelated to the 22 Ma metamorphism in the hanging wall.

Notwithstanding the large proportion of inherited monazite in the Lake Roe schist, the metamorphic ages of the sillimanite-grade schists in Fiordland and the sillimanite-grade paragneisses in Westland agree well. Hence, it would appear that the sillimanite-grade event (M1) is of regional character in the Western Province. Moreover, it was probably related to, or at least occurred simultaneously with, the Karamea-type intrusions.

Kyanite-grade metamorphism (M2) at 330 Ma in Fiordland represents a previously unrecognized period of orogenesis in the Western Province. This event manifests itself not only in monazites from pelitic and psammitic schists, but is also recorded in zircons from quartzofeldspathic orthogneisses. These data indicate a major regional thermal event in the Western Province. Kyanite-grade metamorphic rocks are not widely developed in the Westland-Nelson region although this probably reflects the shallower crustal levels exposed there, as opposed to Fiordland. This age is represented by granites in Westland at Cape Foulwind and Windy Point (Muir *et al*., 1994; Fig. 1).

The monazite ages indicate that the Tuhua sequence was already at high grade by the end of the Palaeozoic. The emplacement of the WFO granulites is a major event in the geological history of Fiordland. The close proximity of the high-grade metamorphic cover sequence has resulted in geological interpretations based on coeval metamorphism of WFO and cover sequence. We have shown that these high-grade metamorphic rocks are not related. Cretaceous thermal disturbance of the zircon U–Pb system is evident in many parts of the cover sequence in Fiordland, such as that exemplified in the Deep Cove Gneisses from Kellard Point, but the exact cause remains uncertain. Other Tuhua-sequence samples analysed in this study derive from areas relatively free of Cretaceous deformation, and so have largely escaped the complications

associated with this later metamorphism. In these areas, Cretaceous deformation has been partitioned into relatively narrow shear zones, leaving large tracts of the Tuhua sequence una ected. Consequently, monazites in these regions retain their Palaeozoic ages.

P–T–t Path for Palaeozoic metamorphism in Fiordland

Combining the thermobarometric data with the zircon and monazite ages permits the determination of a *P–T–t* path for the Tuhua sequence of Fiordland. The most significant feature of this *P–T–t* path (Fig. 14) is its anticlockwise nature consistent with an abrupt increase in pressure accompanying or immediately following crustal thickening. Kyanite-grade metamorphism followed shortly after the sillimanite-grade event (within *c.* 30 Ma) and points to a hitherto unrecognised episode of crustal thickening in New Zealand during the Palaeozoic. However, whether crustal thickening occurred in response to tectonic or magmatic loading is not immediately clear although the former seems more likely given the nature of the regional D2 folds, which are isoclinal and recumbent (Oliver, 1980; Gibson, 1990; 1992). On the other hand, it is interesting to note the coincidence in the age of kyanite-grade metamorphism in Fiordland and the intrusion of Carboniferous granites (Cape Foulwind, Windy Point) in both Westland (Muir *et al.*, 1994), and Fiordland.

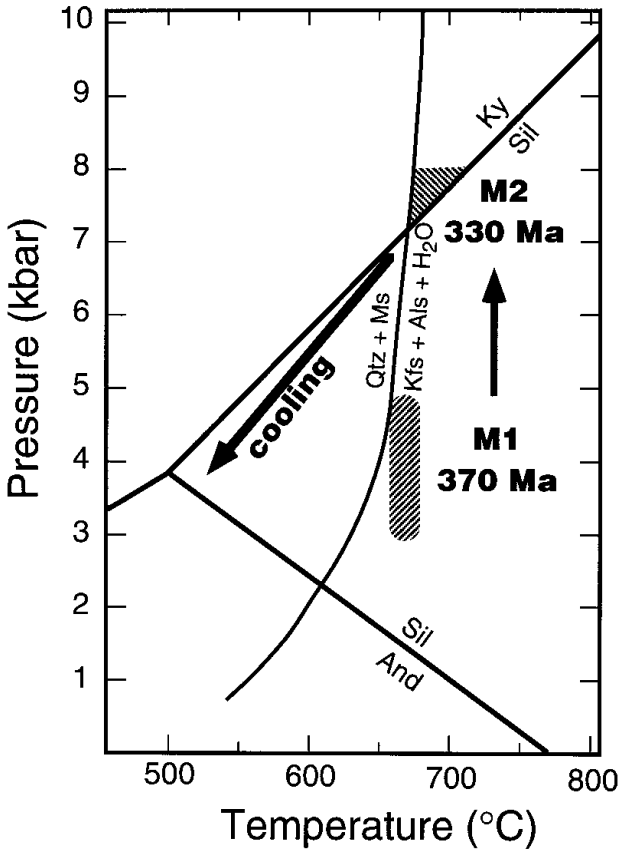

Fig. 14. *P–T*-time path for lower crustal elements in Tuhua sequence that underwent both M1 and M2 metamorphism. Peak *P–T* conditions for M2 metamorphism determined from GASP geobarometer (Ghent, 1976) and observation that kyanite coexists with K-feldspar rather than muscovite at deeper levels of Tuhua sequence. Cooling path constrained by late (post-M2) growth of fibrolitic sillimanite and subsequent replacement of Al_2SiO_5 by staurolite and muscovite. Aluminosilicate phase diagram after Holdaway (1971); breakdown curve for muscovite after Holland (1979).

SUMMARY AND CONCLUSIONS

An outstanding problem in the development of New Zealand continental crust has been the protoliths for the high-grade gneisses. Detrital zircon spectra are consistent with pelitic schists and gneisses being derived from Lower Palaeozoic sedimentary rocks from the Gondwana margin. The Charleston orthogneiss is derived primarily from Separation–Point–Suite granite, with its ultimate metamorphism coincident with the intrusion of the Buckland Granite. Thus, no evidence for older, high-grade basement in New Zealand underlying the sedimentary sequences in the Western Province remains.

Ion microprobe dating of monazite has been used to constrain ages of metamorphism in high-grade metamorphic rocks. The data are summarized in Fig. 15. Three episodes of high-grade metamorphism are distinguished in the Western Province of New Zealand.

- The oldest metamorphic event (*c.* 360 Ma) is of low-*P*/high-*T* type and is common to both the Fiordland and NW Nelson regions; peak metamorphism produced sillimanite–K-feldspar assemblages in rocks of pelitic composition. This event probably occurred in response to intrusion of Devonian granites, such as those in the Karamea Batholith and equivalents in Fiordland.
- The second Palaeozoic event occurred under medium-pressure conditions, giving rise to kyanite-bearing assemblages throughout western Fiordland. Monazites from two M2 kyanite schists indicate an age of 330 Ma. This metamorphic episode may be a response to structural or magmatic thickening or some combination of both.
- The third major metamorphism in New Zealand occurred in the Early Cretaceous (*c.* 125–110 Ma). In Westland, orthogneisses with Separation Point Suite chemistry were emplaced and metamorphosed at *c.* 110 Ma, contemporaneously with intrusion of the Rahu Suite Buckland Granite. In Fiordland, the WFO, which also has Separation Point Suite chemistry, equilibrated at granulite conditions, and was intruded into a cover sequence already at high metamorphic grade. Cretaceous deformation was largely extensional in origin and resulted in strain being partitioned into shear zones whereas large tracts of the cover sequence were largely una ected by the Cretaceous event.

Ion microprobe dating of monazites has revealed that inheritance of earlier monazite generations is more

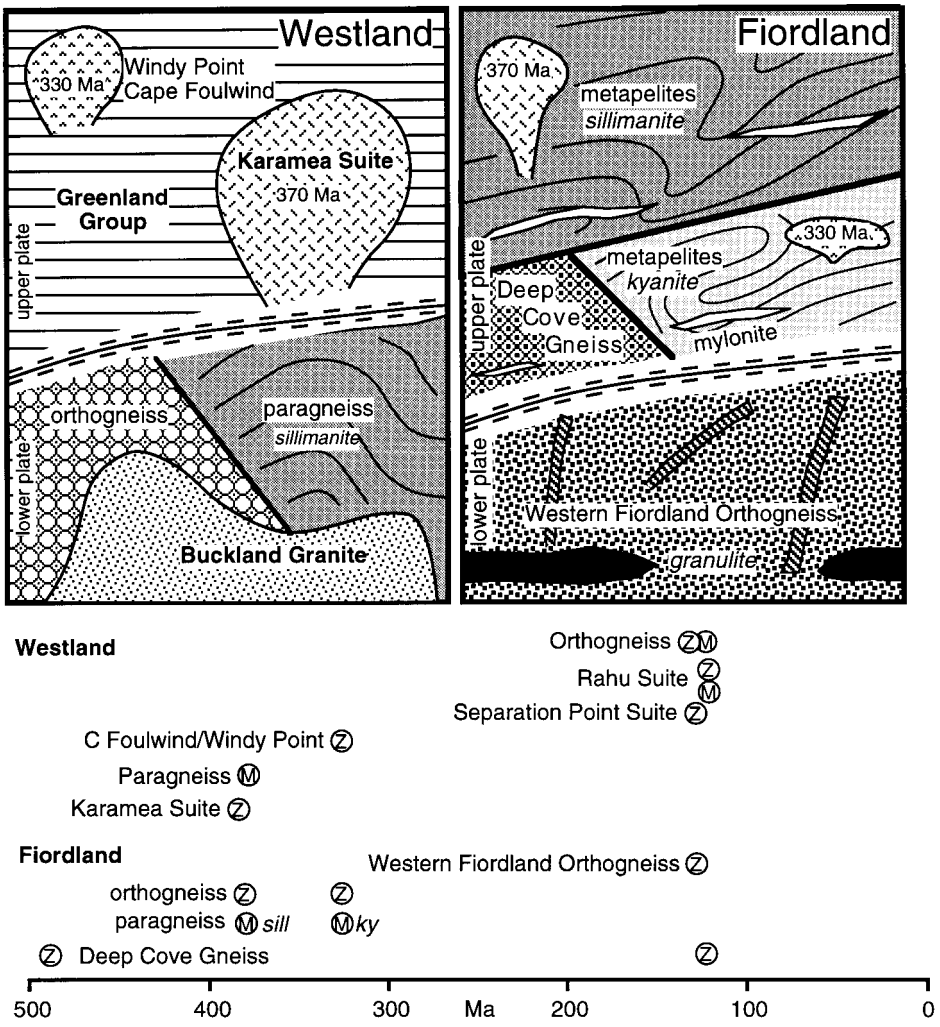

Fig. 15. Summary of relationships (upper) and chronology (lower) of Western Province of New Zealand. Both Westland and Fiordland experienced extension in the mid-Cretaceous, culminating in the development of metamorphic core complexes with exposure of gneisses from mid-lower crustal levels. Detachments are indicated schematically by the annotated line across each section. Z indicates a zircon age; M indicates monazite age.

common than previously thought. Two samples of paragneiss have a large component of metamorphic monazite, but also preserve respectively (a) detrital monazite, and (b) earlier metamorphic monazite. Of course, such features are quite common in zircon. These examples show the utility of the ion microprobe in deconvolving complex metamorphic terranes.

ACKNOWLEDGEMENTS

W. Collins and S. Shaw are thanked for their reviews and R. Vernon is thanked for his editorial e orts. D. Kimbrough and A. Tulloch provided the sample of Charleston orthogneiss. D. Kimbrough's extensive review of an earlier version helped us clarify a number of concepts in this manuscript. W. Premo and M. Fanning are thanked for sharing with us their monazite analyses of the Ma ra adamellite. For accommodation and logistic support in Fiordland, we thank the Deep Cove Education Trust. Permission to collect rock samples in Fiordland National Park was granted by the New Zealand Department of Conservation. Financial support for this project was provided by the Australian Research Council and a travel grant from the University of Southern Queensland (GMG).

REFERENCES

Adams, C. J. D., 1975. Discovery of Precambrian rocks in New Zealand. Age relations of the Greenland Group and Constant Gneiss, West Coast, South Island. *Earth and Planetary Science Letters*, **28,** 98–104.

Aronson, J. L., 1968. Regional geochronology of New Zealand. *Geochimica Cosmochimica Acta*, **32,** 669–697.

Bradshaw, J. Y., 1989. Origin and metamorphic history of an Early Cretaceous polybaric granulite terrain, Fiordland, southwest New Zealand. *Contributions to Mineralogy and Petrology*, **103,** 346–360.

Bradshaw, J. Y., 1990. Geology of crystalline rocks of northern Fiordland: details of granulite facies Western Fiordland

Orthogneiss and associated rock units. *New Zealand Journal of Geology and Geophysics*, **33,** 465–484.
Bradshaw, J. Y. & Kimbrough, D. L., 1989. Age constraints on metamorphism and the development of a metamorphic core complex in Fiordland, southern New Zealand, comment. *Geology*, **17,** 380–381.
Brown, E. H., 1996. High-pressure metamorphism caused by magma loading in Fiordland, New Zealand. *Journal of Metamorphic Geology*, **14,** 441–452.
Cooper, R. A., 1989. Early Palaeozoic terranes in New Zealand. *Journal of the Royal Society of New Zealand*, **19,** 73–112.
Copeland, P., Parrish, R. R. & Harrison, T. M., 1988. Identification of inherited radiogenic Pb in monazite and its implications for U-Pb systematics. *Nature*, **333,** 760–763.
Cumming, G. L. & Richards, J. R., 1975. Ore lead isotope ratios in a continuously changing earth. *Earth and Planetary Science Letters*, **28,** 155–171.
Ghent, E. D., 1976. Plagioclase-garnet-Al_2SiO_5-quartz: a potential geobarometer-geothermometer. *American Mineralogist*, **61,** 710–714.
Ghent, E. D. & Stout, M. Z., 1981. Geobarometry and geothermometry of plagioclase-biotite-garnet-muscovite assemblages. *Contributions to Mineralogy and Petrology*, **76,** 92–97.
Gibson, G. M., 1979. Metamorphites at Wilmot Pass, Fiordland, New Zealand. *Unpubl. PhD Thesis,* Otago University, Dunedin.
Gibson, G. M., 1982. Polyphase deformation and its relationship to metamorphic crystallisation in rocks at Wilmot Pass, Fiordland, New Zealand. *New Zealand Journal of Geology and Geophysics*, **25,** 45–65.
Gibson, G. M., 1990. Uplift and exhumation of middle and lower crustal rocks in an extensional tectonic setting, Fiordland, New Zealand. In: *Exposed Cross-Sections of the Continental Crust* (eds. Salisbury, M. H. & Fountain, D. M.), 71–101. Kluwer Academic, Netherlands.
Gibson, G. M., 1992. Medium-high pressure metamorphic rocks of the Tuhua orogen, western New Zealand as lower crustal analogues of the Lachlan Fold Belt, SE Australia. *Tectonophysics*, **214,** 145–157.
Gibson, G. M. & Ireland, T. R., 1995. Granulite formation during continental extension in Fiordland, New Zealand. *Nature*, **375,** 479–482.
Gibson, G. M. & Ireland, T. R., 1996. Extension of Delamarian (Ross) Orogen into western New Zealand: evidence from zircon ages and implications for crustal growth along the Pacific margin of Gondwana. *Geology*, **24,** 1087–1090.
Gibson, G. M., McDougall, I. & Ireland, T. R., 1988. Age constraints on metamorphism and the development of a metamorphic core complex in Fiordland, southern New Zealand. *Geology*, **16,** 405–408.
Gibson, G. M., McDougall, I. & Ireland, T. R., 1989. Reply to comment on age constraints on metamorphism and the development of a metamorphic core complex in Fiordland, southern New Zealand. *Geology*, **17,** 381–382.
Harrison, T. M. & McDougall, I., 1980. Investigations of an intrusive contact, northwest Nelson, New Zealand: I. Thermal, chronological and isotopic constraints. *Geochimica et Cosmochimica Acta*, **44,** 1985–2003.
Harrison, T. M., McKeegan, K. D. & LeFort, P., 1995. Detection of inherited monazite in the Manaslu leucogranite by $^{208}Pb/^{232}Th$ ion microprobe dating: Crystallization age and tectonic implications. *Earth and Planetary Science Letters*, **133,** 271–282.
Harrison, T. M., Ryerson, F. J., LeFort, P., Yin, A., Lovera, O. & Catlos, E. J., 1997. A late Miocene-Pliocene origin for the Central Himilayan inverted metamorphism. *Earth and Planetary Science Letters*, **146,** E1–7.
Hill, E. J., 1995. A deep crustal shear zone exposed in western Fiordland, New Zealand. *Tectonics*, **14,** 1172–1181.
Holdaway, M. J., 1971. Stability of andalusite and the aluminum silicate phase diagram. *American Journal of Science*, **271,** 97–131.
Holland, T. J. B., 1979. Experimental determination of the reaction Paragonite = Jadite + Kyanite + H_2O and internally consistent thermodynamic data for part of the system Na_2O-Al_2O_3-SiO_2-H_2O, with applications to eclogites and blueschists. *Contributions to Mineralogy and Petrology*, **68,** 292–301.
Ireland, T. R., 1992. Crustal evolution of New Zealand: evidence from age distributions of detrital zircons in Western Province paragneisses and Torlesse greywacke. *Geochimica et Cosmochimica Acta*, **56,** 911–920.
Ireland, T. R., 1995. Ion microprobe mass spectrometry: Techniques and applications in cosmochemistry, geochemistry, and geochronology. In: *Advances in Analytical Geochemistry* (eds Hyman, M. & Rowe, M.), 1–118. JAI Press, Greenwich.
Ireland, T. R., Fanning, C.M., Flöttmann, T., Weaver, S. D., Bradshaw, J. D. & Adams, C., 1995. Continental Structure on the Pacific Margin of Gondwana: Detrital Zircon Ages from Lachlan Fold Belt, Kanmantoo Group and Adelaide Fold Belt of Australia, and Victoria Land Correlatives. *International Antarctic Symposium*, Siena, (abstract), p. 202.
Kimbrough, D. L. & Tulloch, A. J., 1989. Early Cretaceous age of orthogneiss from the Charleston Metamorphic Group, New Zealand. *Earth and Planetary Science Letters*, **95,** 130–140.
Kimbrough, D. L., Tulloch, A. J., Geary, E., Coombs, D. S. & Landis, C. A., 1993. Isotopic ages from the Nelson region of South Island, New Zealand: crustal structure and the definition of the Median Tectonic Zone. *Tectonophysics*, **225,** 433–448.
Kimbrough, D. L., Tulloch, A. J., Coombs, D. S., Landis, C. A., Johnston, M. R. & Mattinson, J. M., 1994. Uranium-lead zircon ages from the Median Tectonic Zone, New Zealand. *New Zealand Journal of Geology and Geophysics*, **37,** 393–419.
Kingsbury, J. A., Miller, C. F., Wooden, J. L. & Harrison, T. M., 1993. Monazite paragenesis and U-Pb systematics in rocks of the eastern Mojave Desert, California: implications for thermochronometry. *Chemical Geology*, **110,** 147–167.
Laird, M. G., 1967. Field relations of the Constant Gneiss and Greenland Group in the Central Paparoa Range, West Coast, South Island. *New Zealand Journal of Geology and Geophysics*, **10,** 247–256.
Landis, C. A. & Coombs, D. S., 1967. Metamorphic belts and orogenesis in southern New Zealand. *Tectonophysics*, **4,** 501–518.
Ludwig, K. R., 1996. Isoplot: A plotting and regression program for radiogenic isotope data. Version 2.91. United States Geological Survey Open-File Report, 91–445.
Mattinson, J. M., Kimbrough, D. L. & Bradshaw, J. Y., 1986. Western Fiordland orthogneiss: Early Cretaceous arc magmatism and granulite facies metamorphism, New Zealand. *Contributions to Mineralogy and Petrology*, **92,** 383–392.
Muir, R. J., Ireland, T. R., Weaver, S. D. & Bradshaw, J. D., 1994. Ion microprobe U-Pb zircon geochronology of granitic magmatism in the Western Province of the South Island, New Zealand. *Chemical Geology (Isotope Geoscience)*, **113,** 171–189.
Muir, R. J., Weaver, S. D., Bradshaw, J. D., Eby, G. N. & Evans, J. A., 1995. Geochemistry of the Cretaceous Separation Point Batholith, New Zealand: granitoid magmas formed by melting of mafic lithosphere. *Journal of the Geological Society, London*, **152,** 689–701.
Muir, R. J., Ireland, T. R., Weaver, S. D. & Bradshaw, J. D., 1996a. Ion microprobe dating of Palaeozoic granitoids: Devonian magmatism in New Zealand and correlations with Australia and Antarctica. *Chemical Geology (Isotope Geoscience)*, **127,** 191–210.
Muir, R. J., Weaver, S. D., Bradshaw, J. D., Eby, G. N., Evans, J. A. & Ireland, T. R., 1996b. Geochemistry of the Karamea Batholith, New Zealand, and comparisons with the Lachlan Fold Belt granites of SE Australia. *Lithos*, **39,** 1–20.
Muir, R. J., Ireland, T. R., Weaver, S. D. and Bradshaw, J. D., Waight, T. E., Jongens, R., and Eby, G. N., 1997. Geochronology of Cretaceous magmatism in NW Nelson-

Westland, South Island, New Zealand. *New Zealand Journal of Geology and Geophysics*, (in press).
Nathan, S., 1976. Geochemistry of the Greenland Group (Early Ordovician), New Zealand. *New Zealand Journal of Geology and Geophysics*, **19,** 683–706.
Newton, R. C. & Haselton, H. T., 1981. Thermodynamics of the garnet-plagioclase-Al_2SiO_5-quartz barometer. In: *Thermodynamics of Minerals and Melts* (eds Newton, R. C., Navrotsky, A. & Wood, B. J.), 131–147. Springer-Verlag, New York.
Oliver, G. J. H., 1980. Geology of the granulite and amphibolite facies gneisses of Doubtful Sound, Fiordland, New Zealand. *New Zealand Journal of Geology and Geophysics*, **23,** 27–41.
Oliver, G. J. H. & Coggon, J. H., 1979. Crustal structure of Fiordland, New Zealand. *Tectonophysics*, **54,** 253–292.
Parrish, R. R., 1990. U-Pb dating of monazite and its application to geological problems. *Canadian Journal of Earth Sciences*, **27,** 1431–1450.
Pickett, D. A. & Wasserburg, G. J., 1989. Neodymium and strontium isotopic characteristics of New Zealand granitoids and related rocks. *Contributions to Mineralogy and Petrology*, **103,** 131–142.
Sambridge, M. S. & Compston, W., 1994. Mixture modeling of multi-component data sets with application to ion-probe zircon ages. *Earth and Planetary Science Letters*, **128,** 373–390.
Shelley, D., 1970. The structure and petrography of the Constant Gneiss near Charleston, South-west Nelson. *New Zealand Journal of Geology and Geophysics*, **13,** 370–391.
Smith, H. A. & Barreiro, B., 1990. Monazite U-Pb dating of staurolite grade metamorphism in pelitic schists. *Contributions to Mineralogy and Petrology*, **105,** 602–615.
Tulloch, A. J., 1983. Granitoid rocks of New Zealand: a brief review. *Geological Society of America Memoir*, **159,** 5–20.
Tulloch, A. J. & Kimbrough, D. L., 1989. The Paparoa Metamorphic Core Complex, New Zealand: Cretaceous extension associated with fragmentation of the Pacific margin of Gondwana. *Tectonics*, **8,** 1217–1234.
Tulloch, A. J. & Palmer K., 1990. Tectonic implications of granite cobbles from the mid-Cretaceous Pororari Group, southwest Nelson, New Zealand. *New Zealand Journal of Geology and Geophysics*, **33,** 205–217.
Tulloch, A. J., Kimbrough, D. L. & Waight, T. E., 1994. The French Creek Granite, North Westland, New Zealand – Late Cretaceous A-type plutonism on the Tasman Passive Margin (extended abstract). In: *Evolution of the Tasman Sea Basin* (eds van der Lingen, G. J., Swanson, K. M. & Muir, R. M.), 65–66. Balkema, Rotterdam.
Turner, F. J., 1937a. The metamorphic and plutonic rocks of Lake Manapouri, Fiordland, New Zealand, Part I. *Transactions of the Royal Society of New Zealand*, **67,** 83–100.
Turner, F. J., 1937b. The metamorphic and plutonic rocks of Lake Manapouri, Fiordland, New Zealand, Part II. *Transactions of the Royal Society of New Zealand*, **67,** 227–249.
Turner, F. J., 1938. The metamorphic and plutonic rocks of Lake Manapouri, Fiordland, New Zealand, Part III. *Transactions of the Royal Society of New Zealand*, **68,** 122–140.
Turner, F. J., 1968. *Metamorphic Petrology, Mineralogical and Field Aspects*. McGraw-Hill, New York.
Waight, T. E., Weaver, S. D., Ireland, T. R., Maas, R., Muir, R. J. & Shelley, D., 1997. Field characteristics and geochronology of the Hohonu Batholith, North Westland, New Zealand. *New Zealand Journal of Geology and Geophysics*, **40,** 1–17.
Watt, G. R., 1995. High-thorium monazite-(Ce) formed during disequilibrium melting of metapelites under granulite-facies conditions. *Mineralogical Magazine*, **397,** 735–743.
Watt, G. R. & Harley, S. L., 1993. Accessory phase controls on the geochemistry of crustal melts and restites produced during water-undersaturated partial melting. *Contributions to Mineralogy and Petrology*, **114,** 550–556.
White, P. J., 1994. Thermobarometry of the Charleston Metamorphic Group and implications for the evolution of the Paparoa Metamorphic Core Complex, New Zealand. *New Zealand Journal of Geology and Geophysics*, **37,** 201–209.
Williams, H., Turner, F. J. & Gilbert, C. M., 1954. *Petrography*. W. H. Freeman and Company, San Francisco.
Williams, I. S. & Claesson, S., 1987. Isotopic evidence for the Precambrian provenance and Caledonian metamorphism of high grade paragneisses from the Seve Nappes, Scandinavian Caledonides II. Ion microprobe zircon U-Th-Pb. *Contributions to Mineralogy and Petrology*, **97,** 205–217.
Williams, I. S., Buick, I. S. & Cartwright, I., 1996. An extended episode of early Mesoproterozoic metamorphic fluid flow in the Reynolds Range, central Australia. *Journal of Metamorphic Geology*, **14,** 29–47.
Williams, I. S., Compston, W. & Chappell, B. W., 1983. Zircon and monazite U-Pb systems and the histories of I-type magmas, Berridale Batholith, Australia. *Journal of Petrology*, **24,** 76–97.

Received 10 December 1996; revision accepted 18 April 1997.

Appendix A—Analytical Details

Isotopic ratios in monazite were formed from the isotopic count rates by using a spline interpolation for time-dependent changes in the denominator count rate and forming ratios at the numerator analysis times. A further correction was based on correlated temporal variations in the Pb/U and UO/U ratios, such that any error associated with movement along the calibration curve can be removed. Outliers were only sought and removed, if warranted, if the initial line fits through the isotopic count rates versus time had very large MSWD values (in excess of 99). Monazite U/Pb and Th/Pb ratios are individually referenced through independent empirical quadratic relationships between Pb/U and UO/U, and Pb/Th and ThO/Th, respectively, and then normalized to the standard. The standard monazite for this work comes from the Ma ra Adamellite of the Lachlan Fold Belt, southeastern Australia (S8624/769549; 36°32′S 138°59′E). Because Ma ra Adamellite monazite has not been used previously, part of this work was to assess the suitability of monazite from this rock in terms of uniformity of U/Pb and Th/Pb ratios.

The potential suitability of the Ma ra Adamellite as a standard was based on concordant K–Ar mica and Rb–Sr mica and U–Pb monazite ages at around 413 Ma (Williams *et al*., 1983). In order to corroborate this age, we analysed a zircon fraction on the SHRIMP I and obtained a U/Pb age of 423.2 ± 4.4 Ma ($2\sigma_m$) which is $2.5 \pm 1.1\%$ older than 413 Ma (Fig. 16). In an attempt to further constrain the age, three fractions of monazite were analysed by M. Fanning and W. Premo using the isotope dilution TIMS facilities at USGS, Denver. Three monazite fractions agree within 1 Ma limits with a mean $^{206}Pb/^{238}U$ age of 421 Ma. We infer that the Williams *et al.* (1983) monazite fractions contain a small fraction of grains that have experienced Pb loss, as is clear in the zircon fractions analysed conventionally as well as by ion microprobe. The new age is still consistent with the field relationships of the surrounding granites (I. S. Williams, person. commun. 1996). The new data pertaining to Ma ra will be presented in detail elsewhere.

In monazite, there appears to be an isobaric interference under the ^{204}Pb peak such that any common Pb correction based on the $^{204}Pb/^{206}Pb$ ratio is an overestimate (Williams *et al*., 1996). Nor can the $^{208}Pb/^{206}Pb$ ratio be used, because ^{208}Pb is dominated by the radiogenic component in monazite (which has per cent levels of Th). Because the subject of this work is Phanerozoic metamorphism, we have used the $^{207}Pb/^{206}Pb$ ratio solely as an estimator of common Pb and then used the $^{206}Pb^*/^{238}U$ and $^{208}Pb^*/^{232}Th$ for age determinations. The ^{207}Pb method assumes that any point (uncorrected for common Pb) on a Tera-Wasserburg concordia diagram is a mixture between a common Pb $^{207}Pb/^{206}Pb$ on the y-axis and a concordant radiogenic composition. By fixing the common Pb composition, an extrapolation to concordia can be made. The common Pb composition is taken as the Cumming & Richards (1975) model Pb composition for the inferred radiogenic age. In most analytical sessions, 20 analyses of the standard were carried

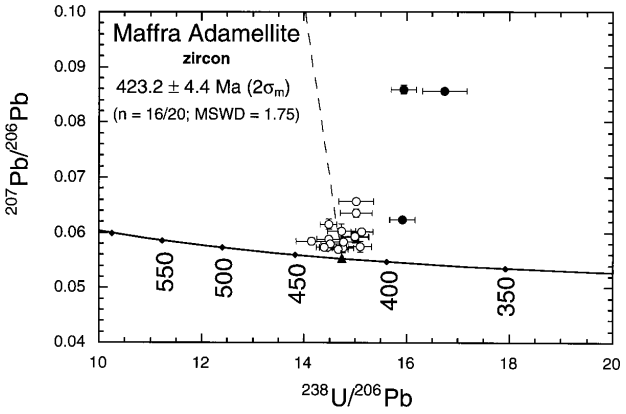

Fig. 16. The standard monazite used for calibrating U–Pb and Th–Pb ratios is from the Ma ra adamellite from southeast Australia. Zircon data are shown on a Tera-Wasserburg concordia plot with uncorrected (for common Pb) Pb isotopic compositions. Each point is projected onto the concordia from the common Pb isotopic composition and the resulting radiogenic $^{206}Pb/^{238}U$ ages are grouped to obtain the mean age. The dashed line indicates the common Pb mixing line between 423.2 Ma common Pb and 423.2 Ma radiogenic Pb (filled triangle). Open symbols are included in the weighted mean; solid symbols are outliers. The weighted mean ion-probe zircon age is in good agreement with the isotope dilution (MSID) values for $^{206}Pb/^{238}U$ in Ma ra monazite from three samples which gives a mean age of 421 ± 1 Ma (unpublished data from C. M. Fanning and W. Premo).

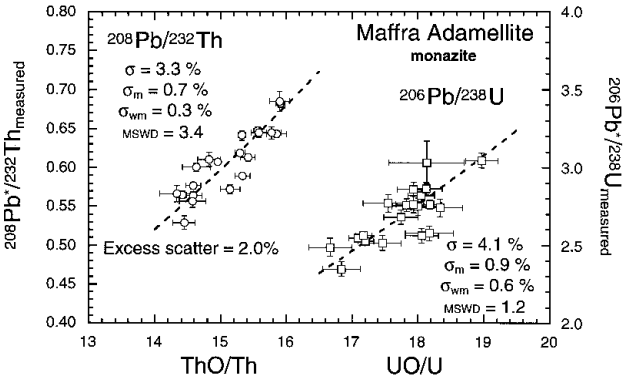

Fig. 17. Examples of calibration curves from Ma ra monazite for Pb–U and Pb–Th systems. These systems are calibrated independently with empirical quadratic relationships ($y = ax^2$) relating $^{208}Pb/^{232}Th$ with ThO/Th, and $^{206}Pb/^{238}U$ with UO/U, respectively. Shown are the statistical parameters for the normalized data: σ, the standard deviation of the population, σ_m, the error of the mean, σ_{wm}, the error of the weighted mean, and MSWD, the mean square of the weighted deviates from the weighted mean. Both U–Pb and Th–Pb systems show similar dispersions, but the higher precision of the Pb–Th measurements (due to the high Th/U of monazite and resultant high ^{208}Pb concentration) reveals excess scatter of 2.0% about the Th–Pb calibration line (MSWD is 3.4 using measurement errors alone). This is ascribed to instrumental discrimination through preferential sputtering related to chemistry or crystal orientation, rather than Pb loss or inheritance, since the compositions determined by mass spectrometric isotope dilution are uniform. This external component of scatter, as obtained from concurrent analyses of the Ma ra standard, is added into the uncertainty of all monazite analyses so as not to interpret analytical scatter as being of geological origin (see Appendix A for discussion).

out. The mean Pb/U and Pb/Th ratios of the 20 standard analyses were pooled and assessed statistically by taking a weighted mean and examining the MSWD about the calibration curve (Fig. 17). Although the mean Pb/U ratio was generally consistent with the individual measurement errors for Ma ra monazite, the mean Pb/Th generally had a high MSWD. This is due to the much higher measurement precision obtained for the Th–Pb system because of the high Th concentration (and resultant high radiogenic ^{208}Pb concentration). The mean was then calculated by assuming that the error of the mean is a combination of the individual measurement errors plus a constant external variance that has a normal distribution (a similar method is used by Ludwig, 1996). For all the standard data sets obtained in this work, the external component is around 2% for the Pb/Th ratios (Fig. 16). Because of a high degree of correlation between the Pb/Th and Pb/U measurements, the external component derived from the Th–Pb system was also used for the Pb–U system. In e ect, the Pb–U variance is masked by the low measurement precision in Ma ra monazite, but the scatter is evident in monazites from other rocks with higher U concentrations. This external variance is possibly a combination of Pb-loss and inheritance in the standards, i.e. it is due to 'geological' error. However, the constancy of this error, and its applicability to the unknowns as well as the standards, suggests that the cause is analytical, possibly due to crystal orientation, chemical di erences, or some other matrix e ect that can cause elemental discrimination (e.g. Ireland, 1995). Such scatter might be ultimately addressed by incorporating another ionic species into the analytical procedure to allow further calibration of the Pb/U and Pb/Th ratios. This has not been attempted as yet.

The external error was factored into the unknowns and the individual analyses were pooled. If the MSWD exceeds the critical value (in this work we use the critical values of the F distribution for n degrees of freedom), outliers were sought. The furthest outlier from the mean was removed first. For most sets, only one or two points were rejected from the mean calculation. The final error of an analysis was derived from the error from the weighted mean of the unknowns, combined with the error in the weighted mean from the standard analyses.

The concentrations of Th and U in Ma ra monazite are highly variable (as indicated by the U and Th count rates) and so no concentrations of unknowns are reported. The Th/U ratio is the measured ThO^+/UO^+ multiplied by a sensitivity factor of 0.84, which is the di erence between the slope of $^{208}Pb^+/^{206}Pb^+$ vs. ThO^+/UO^+ and that predicted for $^{208}Pb/^{206}Pb$ vs. Th/U for the 421 Ma standard.